

1 **Interactions of pathogenic and commensal strains of**  
2 **Mannheimia haemolytica with differentiated bovine**  
3 **airway epithelial cells grown at an air-liquid**  
4 **interface**

5 **Daniel Cozens<sup>1</sup>, Erin Sutherland<sup>1</sup>, Miquel Lauder<sup>1</sup>, Geraldine Taylor<sup>2</sup>, Catherine C.**  
6 **Berry<sup>3</sup> and Robert L. Davies<sup>1\*</sup>.**

7

8 *<sup>1</sup> Institute of Infection, Immunity and Inflammation, College of Medical, Veterinary and Life*  
9 *Sciences, University of Glasgow, Glasgow, UK*

10 *<sup>2</sup> The Pirbright Institute, Pirbright, Surrey, UK*

11 *<sup>3</sup> Institute of Molecular, Cell and Systems Biology, College of Medical, Veterinary and Life*  
12 *Sciences, University of Glasgow, Glasgow, UK*

13

14

15 \*Corresponding Author

16 Email: robert.davies@glasgow.ac.uk

17

18 **Abstract**

19 *Mannheimia haemolytica* serotype A2 is a common commensal species present in the  
20 nasopharynx of healthy cattle. However, prior to the onset of bovine pneumonic  
21 pasteurellosis, there is sudden increase in *M. haemolytica* serotype A1 within the upper  
22 respiratory tract. The events during this selective proliferation of serotype A1 strains are  
23 poorly characterised. In this investigation, a differentiated bovine airway epithelial cell  
24 culture was used to study the interactions of A1 and A2 bovine isolates with the respiratory  
25 epithelium. This model reproduced the key defences of the airway epithelium, including tight  
26 junctions and mucociliary clearance. Although initial adherence of the serotype A1 strains  
27 was low, by 12 hours post-infection the bacteria was able to traverse the tight junctions to  
28 form foci of infection below the apical surface. The size, density and number of these foci  
29 increased with time, as did the cytopathic effects observed in the bovine bronchial epithelial  
30 cells. Penetration of *M. haemolytica* A1 into the sub-apical epithelium was shown to be  
31 through transcytosis but not paracytosis. Commensal A2 bovine isolates however were not  
32 capable of colonising the model to a high degree, and did not penetrate the epithelium  
33 following initial adherence at the apical surface. This difference in their ability to colonise the  
34 respiratory epithelium may account for the sudden proliferation of serotype A1 in the onset of  
35 pneumonia pasteurellosis. The pathogenesis observed was replicated by virulent A2 ovine  
36 isolates; however colonisation was 10-fold lower in comparison to bovine A1 strains. This  
37 investigation provides new insight into the interactions of *M. haemolytica* with bovine airway  
38 epithelial cells which are occurring *in vivo* during pneumonia pasteurellosis.

## 39 **Introduction**

40 Bovine respiratory disease (BRD) is a multifactorial condition of cattle that causes significant  
41 economic losses (>\$3 billion annually in the USA alone) to the cattle industry worldwide [1-  
42 3]. The pathogenesis of BRD is complex, involving poorly understood interactions between  
43 various viral and bacterial pathogens and the host; environmental stress is also an important  
44 pre-disposing factor leading to the outbreak of disease [3-6]. Although many of the viral and  
45 bacterial pathogens can potentially cause disease themselves, it is generally accepted that  
46 viral infection often occurs first and predispose cattle to subsequent bacterial infection [3-9].  
47 Pneumonic pasteurellosis is one of the most severe forms of BRD; it is characterized by an  
48 acute lobar fibronectinizing pneumonia or pleuropneumonia and is associated with the  
49 bacterial pathogen *M. haemolytica* [3, 5, 10, 11].

50 *Mannheimia haemolytica* occurs naturally as a commensal in the upper respiratory tract of  
51 healthy cattle [12, 13] but, under circumstances described above, is frequently associated  
52 with disease [1, 10, 12]. The bacterium comprises 12 capsular serotypes [14] but it is widely  
53 recognized that serotype A2 strains are most commonly associated with healthy cattle, where  
54 they reside as commensals in the nasopharynx and tonsils; conversely, serotype A1 (and more  
55 recently A6) strains are mainly responsible for disease [1, 3, 10, 15, 16]. However, in  
56 addition to differences in capsular polysaccharide biochemistry and structure [17, 18],  
57 serotype A1/A6 and A2 strains of *M. haemolytica* represent distinct chromosomal genotypes  
58 [19, 20] and can also be distinguished by differences in their outer membrane protein (OMP)  
59 profiles [21], lipopolysaccharide types [21, 22] and nucleotide sequence variation in various  
60 virulence-associated genes including *lktA* [23], *ompA* [24], *tbpA* and *tbpB* [25], *plpE* [26] as  
61 well as a number of other genes [20]. The upper respiratory tract of healthy cattle is  
62 predominantly colonized by serotype A2 strains but, for reasons that are not clear (but  
63 probably related to stress and/or viral infection), a transition occurs within this

64 microenvironment which leads to a sudden explosive proliferation in the number of serotype  
65 A1/A6 bacteria present and subsequent colonization [1, 3]. This sudden and selective  
66 explosion in the A1/A6 population within the upper respiratory tract leads to the inhalation of  
67 bacteria-containing aerosol droplets into the trachea and lungs and the onset of pneumonic  
68 pasteurellosis [27]. Crucially, the specific bacterial and host factors responsible for the  
69 sudden shift from commensal serotype A2 to pathogenic serotype A1/A6 populations within  
70 the upper respiratory tract are not clear.

71 The leukotoxin (LktA) of *M. haemolytica* plays a central role in the pathogenesis of  
72 pneumonic pasteurellosis and significant attention has been given to understanding the  
73 molecular mechanisms associated with LktA activity within the lung [1, 3, 28, 29]. In  
74 contrast, there has been far less focus on the interactions of *M. haemolytica* with respiratory  
75 airway epithelial cells and events that might account for the sudden proliferation of serotype  
76 A1/A6 bacteria within the upper respiratory tract. A contributing factor to our poor  
77 understanding of early host-pathogen interactions associated with pneumonic pasteurellosis,  
78 and indeed BRD in general, is the lack of physiologically-relevant and reproducible  
79 methodologies with which to study the intricate molecular and immunological interactions  
80 between pathogens and host. Traditionally, submerged, two-dimensional cultures of a single  
81 cell type have been used to investigate interactions of *M. haemolytic* and other BRD  
82 pathogens within the bovine respiratory tract [30-32] but these have numerous limitations:  
83 they do not reflect the multicellular complexity of the parental tissue *in vivo*, they lack its  
84 three-dimensional (3-D) architecture, and the physiological conditions are not representative  
85 of those found within the respiratory tract. However, these characteristics that are lacking in  
86 submerged cultures can be recapitulated using differentiated airway epithelial cells (AECs)  
87 grown at an air-liquid interface (ALI) and, in recent years, such cell culture approaches have

88 been used to study the interactions of various bacterial and viral pathogens with different host  
89 species [33-43].

90 We have previously investigated the growth conditions required for optimal growth and  
91 differentiation of bovine bronchial epithelial cells at an ALI [44] and assessed the temporal  
92 differentiation of these cells to identify an optimum window suitable for infection studies  
93 [45]. The aim of the present study was to investigate the interactions of a panel of *M.*  
94 *haemolytica* isolates, representing virulent and commensal strains recovered from both cattle  
95 and sheep, with differentiated bovine bronchial epithelial cells grown at an ALI. The course  
96 of infection was followed for up to five days using various microscopic approaches and the  
97 production of selected cytokines measured to ascertain the epithelial cell response.

## 98 **Materials and Methods**

### 99 **Bacterial cultures**

100 Eight wild-type *M. haemolytica* strains (Table 1) isolated from both cattle and sheep were  
101 included in this investigation. The strains were isolated from either pneumonic or healthy  
102 animals. Bacteria were routinely grown on brain-heart infusion (BHI) agar supplemented  
103 with 5% (v/v) defibrinated sheep blood overnight at 37 °C. Broth cultures were grown in  
104 BHI broth at 37 °C with agitation.

### 105 **Culture of bovine bronchial epithelial cells**

106 Bronchial epithelial cells were isolated from cattle aged 24-30 months, as described  
107 previously [44]. Tissue was collected from cattle immediately post-slaughter at Sandyford  
108 Abattoir Ltd., UK. The bronchial tract was swabbed to ensure there was no pre-existing  
109 bacterial or fungal infection. *Ex vivo* bronchi tissue was also collected, fixed in 2% (w/v)  
110 formaldehyde and sectioned for histological analysis to confirm the health of the donor

111 animal. Briefly, the main and lobar bronchi were dissected from the lungs and the  
112 surrounding tissue removed. The BBECs were isolated from the epithelium by incubation  
113 overnight at 4°C in ‘digestion medium’ composed of Dulbecco’s modified Eagle’s medium  
114 (DMEM) and Ham’s nutrient F-12 (1:1) containing 1 mg/ml dithioereitol, 10 µg/ml DNAase  
115 and 1 mg/ml Protease XIV from *Streptomyces griseus*, supplemented with penicillin (100  
116 U/ml), streptomycin (100 µg/ml) and amphotericin (2.5 µg/ml) (Sigma-Aldrich). All  
117 subsequent media, with the exception of media utilised during infection of the BBEC cultures  
118 were also supplemented with penicillin-streptomycin and amphotericin. Digestion of the  
119 bronchial epithelium was halted by the addition of foetal calf serum to give a final  
120 concentration of 10% (v/v). Rigorous rinsing of the luminal surface was used to remove  
121 loosely-attached epithelial cells. The resulting suspension was centrifuged and resuspended  
122 in ‘submerged growth medium’ (SGM), comprised of DMEM/Ham’s F-12 (1:1)  
123 supplemented with 10% (v/v) foetal calf serum. Cells were seeded into T75 tissue culture  
124 flasks ( $5 \times 10^6$  cells/flask) for expansion. The flasks were incubated at 37°C in 5% CO<sub>2</sub> and  
125 14% O<sub>2</sub>, in a humidified atmosphere. At 80-90 % confluency (~4 days post-seeding) the  
126 flasks of BBECs were harvested. Cells were detached using 0.25% trypsin-EDTA solution,  
127 centrifuged and resuspended in SGM at a density of  $5 \times 10^5$  cells/ml. The BBECs were  
128 seeded into the apical chamber of tissue culture inserts (Thincerts, Greiner #66540,  
129 polyethylene terephthalate membrane, 0.4 µm pore diameter,  $1 \times 10^8$  pore per cm<sup>2</sup>) at a  
130 density of  $2.5 \times 10^5$  cells per insert. Cultures were incubated at 37 °C, 5% CO<sub>2</sub>, 14% O<sub>2</sub>, in a  
131 humidified atmosphere. Following overnight incubation, the apical medium of the culture  
132 was removed and the apical surface washed with 0.5 ml PBS to remove unattached cells. The  
133 SGM media in the apical and basolateral compartments was then replaced. This process was  
134 repeated every 2 – 3 days. The trans-epithelial electrical resistance (TEER) of the cultures  
135 were monitored on a daily basis using an EVOM2 epithelial voltohmmeter (World Precision

136 Instruments, UK), as per the manufacturer's instruction. Once the TEER reached above 200  
137  $\Omega/\text{cm}^2$  (~2 days post-seeding) the SGM was replaced with a mixture of SGM and 'air-liquid  
138 interface medium' (ALIM) (1:1). The ALIM was composed of DMEM and airway epithelial  
139 cell growth medium (Promocell) (1:1) supplemented with 10 ng/ml epidermal growth factor,  
140 100 nM retinoic acid, 6.7 ng/ml triiodothyronine, 5  $\mu\text{g}/\text{ml}$  insulin, 4  $\mu\text{l}/\text{ml}$  bovine pituitary  
141 extract, 0.5  $\mu\text{g}/\text{ml}$  hydrocortisone, 0.5  $\mu\text{g}/\text{ml}$  epinephrine and 10  $\mu\text{g}/\text{ml}$  transferrin (all  
142 Promocell). When the TEER value was above 500  $\Omega \text{ cm}^2$  (~6 days post-seeding), an ALI  
143 was generated by removing the medium in the apical compartment, thereby exposing the  
144 epithelial cells to the atmosphere (day 0 post-ALI). Following the formation of the ALI, the  
145 cells were fed exclusively from the basal compartment with ALIM. Apical washing, basal  
146 feeding and TEER measurements were performed every 2 - 3 days until day 21 post-ALI.

#### 147 **Infection of bovine bronchial epithelial cells**

148 The BBEC cultures were infected on day 21 post-ALI. The apical and basal compartments  
149 were washed twice with PBS, 24 hours prior to infection. The cultures were subsequently fed  
150 with 1 ml ALIM with the omission of penicillin-streptomycin and amphotericin. Bacteria  
151 used in the infection were collected from fresh overnight plate cultures, grown in BHI broth  
152 to exponential phase, and resuspended in PBS at  $10^9$  cfu/ml. The bacterial suspension was  
153 used to inoculate the BBEC cultures apically. Each insert was inoculated with 25  $\mu\text{l}$  of  
154 bacterial suspension ( $2.5 \times 10^7$  cfu/insert). Cultures were incubated at 37 °C until the stated  
155 time point post-infection. For infection of undifferentiated BBECs, cultures were infected at  
156 day 0 post-ALI.

#### 157 **Quantification of bacterial adhesion**

158 At stated time points following infection, a viability count was performed on the adherent *M.*  
159 *haemolytica*. The ALIM was removed from the basal compartment and the apical surface of  
160 the transwell was washed three times with 1 ml PBS. The three washes were subsequently

161 pooled and the number of viable bacteria was also assessed. The BBEC were incubated in  
162 0.5 ml PBS with 1% Triton X-100 to permeabilise the epithelial cells. The membrane was  
163 scraped to mechanically disintegrate the culture. Viable bacteria in the lysate and apical  
164 washes were quantified using 10-fold serial dilutions, performed in triplicate, and plating on  
165 BHI agar with 5% (v/v) defibrinated sheep blood, using the Miles and Misra method. Plates  
166 were incubated for six hours at 37 °C and the number of colony-forming units (CFU)  
167 counted. Bacterial number was expressed as a percentage of the inoculum. For the  
168 gentamicin protection assay, the apical surface was treated with 200 µg/ml gentamicin for  
169 one hour at 37 °C prior to permeabilisation. For each animal, bacterial adherence was  
170 quantified in three independent BBEC cultures at all time points.

#### 171 **Histology and immunohistochemistry**

172 At the stated time points post-infection, cultures were fixed by incubation with 4% (w/v)  
173 paraformaldehyde for 15 min at room temperature and rinsed in PBS. The samples were  
174 subsequently dehydrated using a series of increasing ethanol concentrations, cleared with  
175 xylene and infiltrated with paraffin wax. Sections of the wax blocks were cut at 2.5 µm  
176 thickness using a ThermoShandon Finesse ME+ microtome. Samples were stained with  
177 haematoxylin and eosin (H&E) using standard histological techniques. Further sections were  
178 stained for immunohistochemistry. Rabbit anti-bovine OmpA antibody was used to identify  
179 bovine *M. haemolytica* strains and rabbit anti-ovine OmpA antibody was used to identify  
180 ovine *M. haemolytica* strains, at a dilution of 1:800. Heat-induced epitope retrieval was  
181 performed using a Menarini Access Retrieval Unit and staining conducted using a Dako  
182 Autostainer. Endogenous peroxidase was blocked with 0.3% (v/v) H<sub>2</sub>O<sub>2</sub> in PBS. Following  
183 incubation with the primary antibody, binding was identified by application of an anti-rabbit  
184 HRP-labelled polymer and visualization with a REAL EnVision Peroxidase/DAB+ Detection  
185 System (Dako; #K3468). Samples were subsequently counterstained with Gill's



186 haematoxylin, dehydrated, cleared and mounted in synthetic resin before sectioning. Tissue  
187 sections were viewed with a Leica DM2000 microscope.

### 188 **Immunofluorescence microscopy**

189 At the stated time points post-infection, cultures were fixed by incubation with 4% (w/v)  
190 paraformaldehyde for 15 min at room temperature and rinsed in PBS. Samples were  
191 immunofluorescently stained as described previously [44]. Briefly, samples were  
192 permeabilised using permabilization buffer (PBS with 0.5% [v/v] Triton X-100, 100 ml/ml  
193 sucrose, 4.8 mg/ml HEPES, 2.9 mg/ml NaCl and 600 µg/ml MgCl<sub>2</sub>, pH 7.2) for 10 min at  
194 room temperature. Samples were blocked by incubation with PBS containing 0.05% (v/v)  
195 Tween-20, 10% (v/v) goat serum and 1% (w/v) bovine serum albumin. The primary-  
196 secondary antibody pairings were applied as follows. Bovine *M. haemolytica* strains were  
197 detected using *M. haemolytica* antisera produced in cattle (1:50 dilution) and visualised with  
198 goat anti-bovine-FITC antibody (1:400, Thermo Fisher #A18752). Ovine *M. haemolytica*  
199 strains were detected using rabbit anti-ovine OmpA antibody (1:50 dilution) and visualised  
200 with goat anti-rabbit-Alexa Fluor 488 (1:400 dilution; Thermo Fisher; #A-11008). Ciliated  
201 cells were detected with mouse anti-β-tubulin antibody (1:50 dilution; Abcam; #ab131205).  
202 Tight-junction formation was detected with mouse anti-ZO-1 antibody (1:50 dilution;  
203 Thermo Fisher; #33910). Both anti-β-tubulin and anti-ZO-1 antibody binding was detected  
204 with anti-mouse-Alexa Fluor 568 (1:400 dilution; Thermo Fisher; #A-11031). The cultures  
205 were incubated with antibodies diluted in blocking buffer for 1 h at room temperature.  
206 Samples were washed three times in PBS containing 0.05% (v/v) Tween-20 for 2 min  
207 following each incubation. Blocking was repeated after each primary-secondary pairing.  
208 Nuclei were stained with 300 nM 4',6 diamidino-2-phenylindole (DAPI) for 10 min.  
209 Following staining, membranes were cut from their insert and mounted in Vectashield  
210 mounting medium (Vector Laboratories). Samples were observed on a Leica DMI8

211 microscope. Z-stack orthogonal representation was observed on a Zeiss AxioObserver  
212 ZIspinning disk confocal microscope. Analysis of captured images was performed using  
213 ImageJ software.

#### 214 **Scanning electron microscopy**

215 At the stated time points following infection, cultures were fixed in 1.5% (v/v)  
216 glutaraldehyde in 0.1 M sodium cacodylate buffer for 1 h at 4°C. Samples were subsequently  
217 rinsed three times with 0.1 M sodium cacodylate buffer and post-fixed in 1% (w/v) osmium  
218 tetroxide for 1 h at room temperature. The cultures were washed three times for 10 min with  
219 distilled water, stained with 0.5% (w/v) uranyl acetate for 1 h in the dark, washed twice with  
220 distilled water and dehydrated through a series of increasing ethanol concentrations. The  
221 samples were further dehydrated in hexamethyldisilazane before being placed in a desiccator  
222 overnight. Membranes were cut from the inserts, mounted onto aluminium SEM stubs and  
223 gold sputter-coated. The cultures were analysed on a Jeol 6400 scanning electron microscope  
224 at 10 kV.

#### 225 **Results**

##### 226 ***M. haemolytica* infection of undifferentiated bovine bronchial epithelial cells**

227 The ability of *M. haemolytica* to adhere and colonise BBECs was first determined using  
228 undifferentiated cultures. These cultures consisted of primary isolated BBEC cultures grown  
229 in tissue culture inserts under submerged conditions. We have previously shown that under  
230 these conditions BBEC form undifferentiated monolayers. Staining for  $\beta$ -tubulin was  
231 indicative of cytoskeletal microtubules as opposed to cilia staining (Fig S1). However the  
232 cultures did possess tight junctions, as identified using marker Zona Occludens-1 (ZO-1) (Fig  
233 S2).

234 The undifferentiated BBEC cultures were apically infected with either *M. haemolytica* strain  
235 PH2, an A1 serotype isolated from the lung of a pneumonic animal, or PH202, an A2  
236 serotype isolated from the nasopharynx of a healthy animal. Adhesion and colonisation of  
237 the bacteria was quantified following infection (Fig 1A). Initial adherence at 0.5-2 hours  
238 post-infection (hpi) was comparable between the virulent PH2 strain and the commensal  
239 PH202 strain. Approximately 1% of the inoculum initially adhered to the BBECs (Fig 1A  
240 [i]). The majority of the inoculum was present in the apical washes (Fig 1A [ii]). At 24 hpi,  
241 there is a significant increase in the number of PH2 present in the culture, particularly the  
242 number of adherent bacteria (Two-way ANOVA), indicating that the strain was capable of  
243 highly colonising undifferentiated BBECs. This colonisation was not replicated by PH202;  
244 there was not a significant increase in either the number of adherent bacteria or bacteria  
245 removed from the monolayer in the apical wash.

246 The localisation of bacteria adherent to undifferentiated BBECs was detected by labelling  
247 with antisera raised against *M. haemolytica*. Epithelial cells were identified using  $\beta$ -tubulin  
248 and DAPI (Fig 1B and Fig S1). Between 0.5-2 hpi, adherence was low for both strains. A  
249 small population of bacteria was distributed on the apical surface of cells; however several  
250 cultures were visually devoid of adherent bacteria. Conversely, after 24 hpi, PH2 was near-  
251 confluent at numerous foci of infection present across the culture. These foci were separated  
252 by areas of much lower colonisation density. This pattern was not replicated by PH202,  
253 which at 24 hpi continued to show little to no evidence of adherence. Infected BBEC  
254 cultures were also labelled for tight junctional protein ZO-1 to identify the effect of *M.*  
255 *haemolytica* on tight junction integrity (Fig 1C). Tight junctions were shown to be stable  
256 across all time points following infection with PH2 and PH202. However, at the foci of  
257 infection, where PH2 was present at high number, tight junctions could not be observed. This  
258 was determined to be due to damage to the colonised epithelial cells resulting in a disruption

259 in the integrity of the monolayer as opposed to direct targeting of the tight junction by PH2.

260 This will be discussed in greater detail below.

### 261 ***M. haemolytica* infection of differentiated bovine bronchial epithelial cells**

262 Adherence and colonisation of *M. haemolytica* was further determined using differentiated  
263 BBEC cultures. Primary BBEC were grown at an ALI in order to stimulate polarisation of  
264 airway epithelial cells into a culture which closely replicates the *in vivo* epithelium of the  
265 bovine respiratory tract (Fig 2). At 21 days post-ALI, the BBEC cultures were shown to form  
266 a pseudostratified columnar epithelium highly reminiscent to *ex vivo* tissue section (Fig 2A  
267 [i] & 2B [i]). The apical surface of the BBEC cultures displayed both a high degree of  
268 ciliation (Fig 2B [ii] & 2C [i]), and the formation of tight junction (Fig 2C [ii]), characteristic  
269 of the bovine airway lumen. This model has previously been well characterised and was  
270 shown to replicate other hallmarks of the airway epithelium, including the differentiation of  
271 mucus-producing goblet cells and active mucociliary clearance.

272 The differentiated BBEC cultures were infected apically with either PH2 or PH202. The  
273 number of bacteria present in the culture was quantified using the Miles and Misra method at  
274 time points over a five day period (Fig 3). For both PH2 and PH202, initial adherence (0.5-2  
275 hpi) was approximately 1% of the inoculum (Fig 3A); with the majority of the bacteria  
276 removed following apical washing of the BBEC culture (Fig 3B). The number of adherent  
277 PH2 increased within the BBEC cultures in a time-dependent manner from 6 hpi onwards  
278 (Fig 3A). At 24 hpi, the number of PH2 adherent to the model was approximately 1800% the  
279 initial inoculum. There was a subsequent decrease in the number of adherent PH2 at 48 hpi.  
280 It is hypothesised that this decrease was due to removal of damaged BBECs following apical  
281 washing, as discussed below. This increase in the number of adherent PH2 over time was  
282 accompanied by an increase in the number of bacteria removed in the apical wash (Fig 3B).  
283 Conversely, PH202 was not capable of colonising the BBEC model. In cultures derived from

284 two of the three donor animals, no viable bacteria could be detected at 120 hpi. In BBEC  
285 cultures derived from a third animal, PH202 adhered to the culture at approximately 15% the  
286 initial inoculum, 100-fold lower than the virulent PH2 strain (Fig 3A). This trend is  
287 replicated in the number of bacteria removed by the apical wash (Fig 3B).

### 288 ***M. haemolytica* form foci of infection in differentiated bovine bronchial epithelial cells**

289 The distribution of *M. haemolytica* following infection of differentiated BBEC was  
290 determined using several microscopic techniques (Fig 4 & 5). The adhesion of bacteria to the  
291 apical surface was detected by labelling with antisera raised against *M. haemolytica*. From  
292 0.5-6 hpi, PH2 was shown to be distributed across the apical surface of the culture at a low  
293 density (Fig 4A & S3). The bacteria did not display a preference for ciliated or non-ciliated  
294 cells during initial adherence. This observation was confirmed using SEM (Fig 4B & S4).  
295 At 12 hpi, PH2 became increasing abundant at the apical surface, forming focal areas of  
296 infection (Fig 4A [ii]). By this time point, PH2 had penetrated below the apical surface of the  
297 BBEC cultures, as shown in histological sections labelled for *M. haemolytica* using an anti-  
298 OmpA antibody (Fig 4C & S5). The density of PH2 at the foci of infection increased at 16  
299 hpi (Fig 4A [iii]). These foci could be observed using SEM, in which PH2 was present in  
300 near-confluent consolidations below the apical surface (Fig 4B [iii]). Bacteria could not be  
301 observed at the apical surface in the proximity of the foci. Within the histological sections,  
302 PH2 at the foci were shown to have penetrated the entirety of the epithelium to the basal  
303 surface (Fig 4C [iii]). As exposure time increased, the number, size and density of the foci  
304 increased. This phenomenon coincides with an increased quantity of bacteria recovered from  
305 the apical surface (Fig 3A). By 24 hpi, foci were present at high numbers across the culture,  
306 with large regions heavily colonised by PH2 below the apical surface (Fig 4C [v]). The  
307 BBECs neighbouring the foci of infection did not display evidence of damage or cell death in  
308 the initial 24 hours following challenge by PH2.

309 This pattern of infection observed following challenge of differentiated BBEC cultures by  
310 virulent strain PH2 was not mimicked by commensal strain PH202 (Fig 5). The adherence of  
311 PH202 could often be barely detected on the apical surface using immunofluorescence  
312 labelling (Fig 5A) or SEM (Fig 5B). When PH202 was detected within the culture, the  
313 bacteria were present on the apical surface at a low population density. Histological sections  
314 of infected tissue confirmed that PH202 was not capable of penetrating the apical surface of  
315 the culture (Fig 5C).

316 The effect of apical infecting with PH2 or PH202 on the integrity of the BBEC cultures was  
317 investigated in histological sections (Fig 6 and S6). A semi-quantitative assessment of the  
318 degree of infection was conducted at each time point from cultures derived from three  
319 individual animals (Table 2). Evidence of infection following challenge by PH2 could be  
320 observed by 12 hpi, at which individual foci of infection could be observed in regions across  
321 the culture. The foci were increasingly abundant by 24 hpi. The BBECs at these foci  
322 displayed cytopathic effects. Airway epithelial cells colonised by high numbers of PH2  
323 became increasingly rounded and detached from the epithelium (Fig 6 [v]). Infected cells  
324 displayed cytoskeletal staining for  $\beta$ -tubulin as opposed to cilia, indicating the cells are  
325 becoming dedifferentiated. By 48 hpi, the integrity of the epithelium was drastically reduced,  
326 and the majority of the culture was dislodged following apical washing (Fig S6). This may  
327 account for the reduction in CFU at 48 hpi (Fig 3A). Epithelial cells still attached to the  
328 epithelium appeared rounded (Fig S3) and were heavily colonised by bacteria (Fig S4). This  
329 observation was not replicated following infection with PH202. Cultures remained healthy  
330 until the time course was halted at 120 hpi (Fig S6). There was no evidence of cell rounding  
331 or increased cell death, with the exception of animal 1, which at 120 hpi showed reduced  
332 integrity of the cell layer. This was not observed in animal 2 or 3 (Table 2).

333 ***M. haemolytica* cause intracellular infections in differentiated bovine bronchial**  
334 **epithelial cells**

335 Following labelling for PH2 within infected differentiated BBEC cultures, the distribution of  
336 adherent bacteria appeared intracellular (Fig 4A [iv] & [v]). This was also observed in  
337 histological sections (Fig 4C [v]). A gentamicin protection assay was used to confirm this  
338 observation (Fig 7A). Following apical infection by PH2, a small subpopulation of  
339 gentamicin-resistant (internalised) bacteria was enumerated at 12 hpi. This population  
340 significantly increased by 24 hpi ( $p < 0.001$ , Two-way ANOVA). However, by 48 hpi this  
341 number subsequently decreased, which coincided with the reduced integrity of the  
342 epithelium. At this time point, high numbers of extracellular bacteria could be detected  
343 across the remaining tissue (Fig S4). Gentamicin-resistant (internalised) PH202 could not be  
344 detected at any time points following challenge.

345 Confocal microscopy confirmed the presence of intracellular *M. haemolytica* within BBECs  
346 (Fig 7B). Z-stack projections of culture 24 hpi following challenge by PH2 confirmed the  
347 presence of PH2 at near-confluent density confined within cell boundaries of both ciliated  
348 and non-ciliated epithelial cells (Fig 7B). This phenomenon was confirmed using SEM (Fig  
349 7C). Epithelial plasma membrane projections could be observed in proximity to PH2 at the  
350 surface of a non-ciliated epithelial cell, suggesting the bacteria was being internalised via  
351 macropinocytosis (Fig 7C [i]). Internalised bacteria could also be observed at high number  
352 within epithelial cells when the apical membrane was removed (Fig 7C [ii]). This suggested  
353 *M. haemolytica* penetrated the apical surface via transcytosis, and was capable of intracellular  
354 survival within airway epithelial cells.

355 ***M. haemolytica* does not affect tight junction integrity in differentiated bovine bronchial**  
356 **epithelial cells**

357 The integrity of tight junctions between BBECs within infected cultures was assessed  
358 following challenge by PH2 and PH202 (Fig 8). At early time points (0.5-20 hpi), tight  
359 junctions could be observed in the BBEC cultures, there was no detectable effect on the  
360 integrity of the junctional complexes due to colonisation of *M. haemolytica*. This observation  
361 was true for both the foci of infections and cells which were not colonised. Tight junctions  
362 however did appear effected at later time points following challenge by PH2 (24 hpi).  
363 Rounded epithelial cells at the foci of infection displayed reduced integrity of tight junctions  
364 at cell-to-cell borders (Fig 8A [v]). From 48-120 hpi, the epithelium was severely  
365 deteriorated and tight junctions could not be observed (Fig S7). PH202 infection however  
366 had no effect on the presence of tight junctions. These observations were confirmed by the  
367 measuring the TEER of the culture following infection (Fig 8B). Challenge by PH202 had no  
368 detectable effect on the TEER of the culture. Conversely, PH2 caused a significant reduction  
369 in TEER at 48 hpi ( $p < 0.001$ , Two-way ANOVA). This indicated that colonisation by PH2  
370 disturbed the integrity of the tight junctions.

371 This damage to junctional complexes was determined to be due to damage to the epithelium  
372 as opposed to direct targeting of tight junctions by *M. haemolytica*. Lipoxin A4 was used to  
373 stimulate tight junction formation [46]. Following treatment with lipoxin A4, TEER was  
374 increased within the BBEC culture, and labelling for ZO-1 became increasingly prominent, in  
375 a dose-dependent manner (data not shown). It was hypothesised that if PH2 was targeting  
376 tight junctions to penetrate the apical surface to colonise the culture, colonisation would be  
377 reduced following treatment. However, lipoxin A4 pre-treatment of BBECs did not affect the  
378 number of CFU adherent to the culture following challenge by PH2 24 hpi (Fig 8C).



379 **Serotype and host species of origin affects the capacity of *M. haemolytica* to colonise**  
380 **differentiated bovine bronchial epithelial cells**

381 Differentiated BBECs were infected with eight strains of *M. haemolytica*, listed in Table 1.  
382 These strains were isolated from healthy and pneumonic cattle and sheep. Cultures were  
383 infected apically with  $2.5 \times 10^7$  cfu/insert, and colonisation was quantified at 2, 24 and 72 hpi  
384 (Fig 9A [i] & S8). The number of CFU present in the apical wash was also enumerated (Fig  
385 9 [ii] 7 S8). At 2 hpi, there was no significant difference in the adherence efficiency between  
386 all eight strains (Two-way ANOVA). There was little evidence of bacteria present on the  
387 apical surface as observed using SEM at 2 hpi (Fig S10 & S11). By 24 hpi however, both the  
388 virulent A1 and A6 strains isolated from pneumonic cattle (PH2 and PH376 respectively) and  
389 virulent A2 strains isolated from pneumonic sheep (PH278 and PH372) were capable of  
390 successfully colonising the BBEC cultures. This colonisation was observed as foci of  
391 infection below the apical surface, as described for PH2 (Fig 10A). The apical surfaces  
392 surrounding the foci were largely devoid of adherent bacteria (Fig 10B). Adherence of  
393 virulent bovine strains to the BBEC was approximately 10-fold higher in comparison to  
394 virulent ovine strains. This was reflected in a higher number of foci of infection present after  
395 challenge with PH2 and PH376. At 72 hpi, significant deterioration was observed in epithelia  
396 infected by all virulent strains, as displayed within histological sections and SEM (Fig 10).  
397 This was reflected in a reduction in the TEER (Fig 9B). A semi-quantitative scoring of this  
398 damage using histological sections was performed (Table 3). Deterioration following  
399 infection by virulent ovine strains, particularly PH372 was less prominent in comparison to  
400 the bovine strains, which appeared more invasive to BBEC cultures.

401 Neither the commensal bovine (PH202 and PH210, A2 serotype) or ovine strains (PH62 and  
402 PH346, A12 serotype) displayed a significant increases in adherence efficiency between 2 to  
403 24 hpi (Two-way ANOVA; Fig 9). There was a slight increase in CFU present in the culture

404 for all commensal strains by 72 hpi; however the number of bacteria within the culture was  
405 significantly lower in comparison to all strains isolated from pneumonic animals. Visually,  
406 BBEC cultures infected by commensal strains did not present overt evidence of colonisation  
407 or damage to the epithelium (Fig 10), and the TEER was not affected (Fig 9B). Foci of  
408 infection could be observed in individual cultures for PH210, PH62 and PH346 (Table 3).  
409 However these were in isolated incidence and were present at a much lower number in  
410 comparison to virulent strains. Such foci were located towards the border regions of the foci,  
411 at which the epithelium can present evidence of damage. This data suggests that virulent  
412 strains were capable of successfully colonising differentiated BBEC following apical  
413 infection. Conversely, commensal strains isolated from the nasopharynx of healthy animals  
414 were not capable of successfully colonising the model to a high degree.

## 415 **Discussion**

416 The aim of the study was to investigate the interaction between pathogenic and virulent  
417 strains of *M. haemolytica* with the bovine airway epithelium using a differentiated cell model,  
418 in order to have a better understanding of the events of BRD. Differentiated airway epithelial  
419 models have been utilised previously to study a number of bacterial pathogens, including  
420 *Pseudomonas aeruginosa* [47-49], *Haemophilus influenzae* [50-52], *Neisseria meningitidis*  
421 [53] and *Mycoplasma pneumoniae* [38, 41]. To our knowledge, this investigation is the first  
422 to utilise a differentiated cell model to study the interaction of *M. haemolytica* with the  
423 bovine airway epithelium. This has allowed the adherence, colonisation and traversal of the  
424 epithelium by *M. haemolytica* to be studied in a model which displayed the characteristic  
425 defence mechanisms associated with the respiratory tract. The model provides an alternative  
426 to animal models, which are costly and time-intensive, and are contrary to the three R's  
427 principles.

428 Submerged BBECs have routinely been utilised to study the adherence of *M. haemolytica*  
429 [30, 54-56]. However, submerged epithelial cultures are undifferentiated [57], and as such do  
430 not replicate the complexity of the airway epithelium [58]. Bovine bronchial epithelial cells  
431 can be stimulated to differentiate into a more representative model of the *in vivo*  
432 microenvironment through exposure to the atmosphere [36, 37, 59]. The methodology for  
433 differentiation of bovine airway epithelial cells have been fully optimised [44] and the model  
434 well-characterised [45]. The differentiated BBEC model has been shown to replicate the  
435 hallmark defences of the respiratory tract, including active mucociliary clearance. These  
436 mechanisms actively prevent colonisation of invading pathogens, and are important  
437 considerations when modelling bacterial interactions within the airway. Tight junctions  
438 present in the differentiated BBEC also allowed for the identification of invasion of the  
439 pathogen through the apical barrier (Fig 4C) into the sub-apical epithelium. Our model  
440 therefore allows for these defence mechanisms to be considered when assessing colonisation  
441 of *M. haemolytica*, and as such provides an excellent model to characterise *M. haemolytica*-  
442 host interaction in the bovine airway epithelium.

443 A direct comparison of the ability of *M. haemolytica* to colonise differentiated and  
444 undifferentiated BBEC cultures was made in this investigation (Fig 1 & Fig 3). Initial  
445 adherence of *M. haemolytica* to BBEC was comparable between the two models. As  
446 undifferentiated BBEC cultures do not possess cilia, it was inferred that adhesion is not  
447 specific to either ciliated or unciliated cells. This was confirmed using immunofluorescence  
448 and SEM (Fig 4). In both models PH2, isolated from lung of pneumonic cattle, was capable  
449 of heavily colonising cells by 24 hpi. Adherence at 24 hpi was 10-fold higher in the  
450 differentiated model in comparison to the undifferentiated model. This may be due to the  
451 increased thickness of the epithelium in the differentiated model, where a columnar,  
452 pseudostratified morphology was formed, stereotypical for the airway epithelium (Fig 2), as

453 opposed to a two-dimensional monolayer. This provided a larger 3-D architecture for the  
454 bacteria to adhere, highlighting the importance of cell differentiation when investigating  
455 epithelial colonisation.

456 The differentiated BBEC was initially infected with two strains of *M. haemolytica*, PH2, a  
457 bovine isolate from the lung of a pneumonic animal, and PH202, a bovine isolate from the  
458 nasopharynx of a healthy animal (Fig 3). PH2 is an A1 serotype strain, which is the major  
459 cause of pneumonic pasteurellosis in cattle [60, 61]. PH202 is an A2 serotype, a  
460 predominately non-pathogenic serotype present as a commensal species in cattle [29, 61]. A1  
461 and A2 are the most prevalent serotypes worldwide [29, 60]. Both strains have previously  
462 been shown to adhere to undifferentiated ovine bronchial epithelial cells [62]. Initial  
463 adherence of both PH2 and PH202 to differentiated BBEC cultures was low (Fig 3). At early  
464 time points (0.5-6 hpi), bacteria associated with the culture were distributed at a low density  
465 across the apical surface (Figs 4A & 5A). However, following further incubation PH2  
466 became increasingly abundant. Penetration of PH2 below the apical surface of the culture  
467 was identified by 12 hpi; suggesting *M. haemolytica* A1 is capable of traversing epithelial  
468 tight junctions (Fig 4C). This coincided with a significant increase in the number of adherent  
469 bacteria (Fig 3). At the foci of infection, PH2 replicated to a high density below the apical  
470 surface (Fig 4). Such foci have previously been described for *H. influenza* [51] and *M.*  
471 *pneumoniae* [41]. The number of foci increased with exposure time, as did the number of  
472 PH2 present in the systems which were not closely associated with tissue (Fig 3). This  
473 provided evidence that the bacteria disseminated from the foci to re-infecting other regions of  
474 the culture. From 48 hpi onwards, the majority of the epithelium was heavily infected, and  
475 distinct foci no longer observed.

476 Conversely, A2 commensal strain PH202 was not capable of colonising the differentiated  
477 BBEC model. Although initial adherence of the bacterium could be detected at early time

478 points post-infection (Fig 3), there was no evidence of PH202 penetrating the apical surface  
479 (Fig 5C). In tissue derived from two of the three animals, viable PH202 could not be  
480 recovered from the culture at the end point of the infection. This finding indicated that the  
481 differentiated model actively prevented colonisation by the bacteria. This may be due to  
482 mucociliary clearance which actively removes invading pathogens [63, 64]. Alternatively,  
483 BBECs are known to produce anti-bacterial peptides, such as tracheal antimicrobial peptide  
484 (TAP), in response to bacterial products including LPS [65-67]. This peptide has shown to  
485 be bactericidal against *M. haemolytica* [68]. The variation observed in the ability of the A1  
486 and A2 bacteria to adhere to the culture may provide insight into the selective explosion of  
487 the A1 population over A2 strains, resulting in infection in the lower respiratory tract during  
488 pneumonic pasteurellosis [27].

489 Following extended co-culture of differentiated BBECs and PH2 (48-120 hpi), there was  
490 significant evidence of damage present in airway epithelial cells. By 24 hpi, there was cell  
491 rounding and detachment in BBECs heavily colonised by *M. haemolytica* (Fig 6). This  
492 phenomenon was more pronounced at 48 hpi, where a large number of cells were readily  
493 detached from culture following apical washing (Fig S6). This response was only observed  
494 following PH202 infection in tissue derived from one of three animals at 120 hpi (Table 2).  
495 Similar cytopathic effects in epithelial cells have been observed in response to other bacterial  
496 pathogens, including *P. aeruginosa* [69] and *Klebsiella pneumoniae* [70]. This may mimic  
497 events *in vivo*. Clinical signs of *M. haemolytica* include pulmonary lesions, and necrosis and  
498 desquamation can also be observed at the bronchial epithelium [29]. The cause of the  
499 induced cell death in the model is unknown. Major *Mannheimia* virulence factors  
500 lipopolysaccharide (LPS) and leukotoxin have been shown to not cause necrosis or apoptosis  
501 in bovine pulmonary epithelial cells [71]. Epithelial cell death observed in the system may

502 however be due to the innate immune response following bacterial infection, resulting in the  
503 sloughing off of infected cells [72].

504 In this study we presented evidence that *M. haemolytica* A1 strain PH2 may be internalised  
505 by airway epithelial cells following infection (Fig 7). Internalisation of *M. haemolytica* A1  
506 by BBECs has not been previously reported. A small subpopulation of PH2 was identified to  
507 be resistant following treatment with gentamicin, indicative of the presence of intracellular  
508 bacteria (Fig 7A). This was confirmed using a number of microscopy techniques (Figs 7B  
509 and 7C). Within BBECs, intracellular PH2 could be detected from 12 hpi. This number  
510 appeared to peak at 24 hpi (Fig 7A). Electron microscopy suggests that internalisation of  
511 PH2 in epithelial cells may be occurring through macropinocytosis (Fig 7C). This has  
512 previously been observed for *H. influenzae* [51]. *M. haemolytica* was present at high density  
513 within cell boundaries (Fig 7B), suggesting that once internalised PH2 is capable of survival  
514 and replication within host cells. *M. haemolytica* A1 may invade BBECs in order to gain  
515 access to sub-epithelial spaces thorough transcytosis of the epithelium. An intracellular  
516 phase during infection may also allow for persistence or evasion of aspects of host immunity,  
517 such as humoral and complement-attack or mucociliary clearance [73].

518 Tight junctions create a physiochemical barrier to prevent the invasion of pathogens from the  
519 lumen of the airway to the interstitial compartment [74, 75]. However, several bacteria are  
520 capable of disrupting the junctional complexes during paracytosis [76, 77]. This was not  
521 observed following colonisation of either PH2 or PH202 (Fig 8). Tight junctions were  
522 present following challenge by *M. haemolytica*, with no detectable reduction in integrity by  
523 24 hpi (Fig 8A). This was confirmed by measuring the TEER of the culture (Fig 8B). There  
524 was however a detectable decrease in the number of tight junctions present by 48 hpi with  
525 PH2. However this was due to significant damage to the epithelium following infection,  
526 particularly at the apical surface (Fig S6). The addition of lipoxin A4, which stimulates

527 expression of ZO-1, has previously been shown to prevent the invasion and transmigration of  
528 *P. aeruginosa* [78]. However stimulation of BBEC cultures did not prevent colonisation by  
529 PH2, despite enhancing the integrity of tight junctions (Fig 8C), further suggesting that tight  
530 junctions are not targeted by *M. haemolytica*. It is hypothesised therefore that transmigration  
531 of the bacterium through the apical surface of the epithelium occurred via transcytosis, but  
532 not through paracellular transport.

533 The pattern of infection of PH2 was replicated using a bovine A6 isolate PH376. Both strains  
534 colonised the BBEC cultures to a comparable degree (Fig 9A), forming morphologically  
535 similar infection foci (Fig 10) beneath the apical surface at 24 hpi. Significant damage to the  
536 tissue was detected at 72 hpi with both strains (Fig S12). A2 bovine isolate PH210, in  
537 agreement with PH202, was not capable of forming foci of infection stereotypical of A1  
538 strains (Fig 10). The model was further challenged with four ovine isolates (Fig 9 & 10).  
539 Two strains (PH278 and PH372) were representative of A2 ovine strains, the major causative  
540 agent of pneumonia in sheep [29, 60]. As with the bovine isolates, the virulent strains were  
541 capable of colonising the model to form foci of infection. The A2 bovine isolates behaved  
542 differently from ovine A2 isolates when co-cultured with the model (Fig 9). This is to be  
543 expected as the outer-membrane protein profiles differ between the two groups [21].  
544 Cultures were also infected with two A12 strains (PH62 and PH346), which are traditionally  
545 not associated with disease. The commensal A12 strains failed to colonise the cultures to a  
546 similar degree (Fig 9). Adherence to bovine airway epithelial cells by virulent ovine isolates  
547 was approximately 10-fold lower in comparison to virulent bovine isolates (Fig 9). This  
548 suggests that host specificity in *M. haemolytica* strains was partly dependent on specific cell-  
549 surface structures present on differentiated BBECs. This difference in pathogenesis between  
550 serotypes is likely due to variation in the LPS profile [21, 22], outer-membrane proteins [21]  
551 and allelic variation in a number of virulence genes such as *lktA* [23], *ompA* [24]. In

552 conclusion, variation in disease pathogenesis *in vivo* due to serotype and host specificity is  
553 reflected in the degree of colonisation within the differentiated BBEC culture.

554 In this study we have characterised the host-pathogen interactions between BBECs grown at  
555 an ALI with various serotypes of *M. haemolytica*. The model used to investigate the  
556 infection *in vitro* has been shown to be highly representative of the *in vivo* epithelium,  
557 providing insight into the pathogenesis of *M. haemolytica* during pneumonic pasteurellosis in  
558 the context of host defence mechanisms, such as tight junctions and mucociliary clearance.  
559 *M. haemolytica* A1 was capable of highly colonising the model, causing extensive damage to  
560 the host epithelium. This occurred at foci of infection, below the apical surface of the tissue.  
561 Tight junctions in the epithelium were bypassed using transcytosis, but not paracytosis. *M.*  
562 *haemolytica* A2 was not capable of replicating this colonisation. This may account for the  
563 occurrence of lower respiratory tract infection following the shift from A2 to A1 population  
564 in cattle prior to onset of pneumonic pasteurellosis. The BBEC model was further challenged  
565 using a panel of isolates, and the degree of pathogenesis was dependent on both serotype and  
566 host species. This investigation provides the first insight into the route of infection of *M.*  
567 *haemolytica* in a differentiated model of the bovine airway epithelium.

## 568 **Acknowledgements**

569 We thank Ms Margaret Mullin and Ms Lynne Stevenson (both University of Glasgow) for  
570 assistance with electron microscopy and histology, respectively.



571 **References**

- 572 1. Jeyaseelan S, Sreevatsan S, Maheswaran SK. Role of *Mannheimia haemolytica*  
573 leukotoxin in the pathogenesis of bovine pneumonic pasteurellosis. *Anim Health Res Rev.*  
574 2002; 3: 69-82. pmid: 12665107.
- 575 2. Jones C, Chowdhury S. A review of the biology of bovine herpesvirus type 1 (BHV-  
576 1), its role as a cofactor in the bovine respiratory disease complex and development of  
577 improved vaccines. *Anim Health Res Rev.* 2007; 8: 187-205. doi:  
578 10.1017/S146625230700134X. pmid: 18218160.
- 579 3. Singh K, Ritchey JW, Confer AW. *Mannheimia haemolytica*: bacterial-host  
580 interactions in bovine pneumonia. *Vet Pathol.* 2011; 48: 338-48. doi:  
581 10.1177/0300985810377182. pmid: 20685916.
- 582 4. Czuprynski CJ. Host response to bovine respiratory pathogens. *Anim Health Res Rev.*  
583 2009; 10: 141-3. doi: 10.1017/S1466252309990181. pmid: 20003650.
- 584 5. Panciera RJ, Confer AW. Pathogenesis and pathology of bovine pneumonia. *Vet Clin*  
585 *North Am Food Anim Pract.* 2010; 26: 191-214. pmid: 20619179.
- 586 6. Srikumaran S, Kelling CL, Ambagala A. Immune evasion by pathogens of bovine  
587 respiratory disease complex. *Anim Health Res Rev.* 2007; 8: 215-29. doi:  
588 10.1017/S1466252307001326. pmid: 18218162.
- 589 7. Gershwin LJ, Berghaus LJ, Arnold K, Anderson ML, Corbeil LB. Immune  
590 mechanisms of pathogenetic synergy in concurrent bovine pulmonary infection with  
591 *Haemophilus somnus* and bovine respiratory syncytial virus. *Vet Immunol Immunopathol.*  
592 2005; 107: 119-30. doi: 10.1016/j.vetimm.2005.04.004. pmid: 15979157.
- 593 8. Gershwin LJ, Van Eenennaam AL, Anderson ML, McEligot HA, Shao MX, Toaff-  
594 Rosenstein R, et al. Single pathogen challenge with agents of the bovine respiratory disease

- 595 complex. PLoS One. 2015; 10: e0142479. doi: 10.1371/journal.pone.0142479. pmid:  
596 26571015.
- 597 9. Hodgson PD, Aich P, Manuja A, Hokamp K, Roche FM, Brinkman FS, et al. Effect  
598 of stress on viral-bacterial synergy in bovine respiratory disease: novel mechanisms to  
599 regulate inflammation. Comp Funct Genomics. 2005; 6: 244-50. doi: 10.1002/cfg.474. pmid:  
600 18629190.
- 601 10. Rice JA, Carrasco-Medina L, Hodgins DC, Shewen PE. *Mannheimia haemolytica* and  
602 bovine respiratory disease. Anim Health Res Rev. 2007; 8: 117-28. doi:  
603 10.1017/s1466252307001375.
- 604 11. Whiteley LO, Maheswaran SK, Weiss DJ, Ames TR, Kannan MS. *Pasteurella*  
605 *haemolytica* A1 and bovine respiratory disease: pathogenesis. J Vet Intern Med. 1992; 6: 11-  
606 22. pmid: 1548621.
- 607 12. Confer AW. Update on bacterial pathogenesis in BRD. Anim Health Res Rev. 2009;  
608 10: 145-8. doi: 10.1017/S1466252309990193. pmid: 20003651.
- 609 13. Frank GH. Pasteurellosis of cattle. In: Adlam C, Rutter JM, editors. *Pasteurella* and  
610 Pasteurellosis. London: Academic Press; 1989. p. 197-222.
- 611 14. Angen O, Muters R, Caugant DA, Olsen JE, Bisgaard M. Taxonomic relationships of  
612 the [*Pasteurella*] *haemolytica* complex as evaluated by DNA-DNA hybridizations and 16S  
613 rRNA sequencing with proposal of *Mannheimia haemolytica* gen. nov., comb. nov.,  
614 *Mannheimia granulomatis* comb. nov., *Mannheimia glucosida* sp. nov., *Mannheimia*  
615 *ruminalis* sp. nov. and *Mannheimia varigena* sp. nov. Int J Syst Bacteriol. 1999; 49 Pt 1: 67-  
616 86. doi: 10.1099/00207713-49-1-67. pmid: 10028248.
- 617 15. Griffin D, Chengappa MM, Kuszak J, McVey DS. Bacterial pathogens of the bovine  
618 respiratory disease complex. Vet Clin North Am Food Anim Pract. 2010; 26: 381-94. doi:  
619 10.1016/j.cvfa.2010.04.004. pmid: 20619191.

- 620 16. Klima CL, Alexander TW, Read RR, Gow SP, Booker CW, Hannon S, et al. Genetic  
621 characterization and antimicrobial susceptibility of *Mannheimia haemolytica* isolated from  
622 the nasopharynx of feedlot cattle. *Vet Microbiol.* 2011; 149: 390-8. doi:  
623 10.1016/j.vetmic.2010.11.018. pmid: 21146332.
- 624 17. Adlam C, Knights JM, Mugridge A. Production of colomic acid by *Pasteurella*  
625 *haemolytica* serotype A2 organisms. *FEMS Microbiol Lett.* 1987; 42: 23-5.
- 626 18. Adlam C, Knights JM, Mugridge A, Lindon JC, Baker PR, Beesley JE, et al.  
627 Purification, characterization and immunological properties of the serotype-specific capsular  
628 polysaccharide of *Pasteurella haemolytica* (serotype A1) organisms. *J Gen Microbiol.* 1984;  
629 130: 2415-26. doi: 10.1099/00221287-130-9-2415. pmid: 6502135.
- 630 19. Davies RL, Arkinsaw S, Selander RK. Evolutionary genetics of *Pasteurella*  
631 *haemolytica* isolates recovered from cattle and sheep. *Infect Immun.* 1997; 65: 3585-93.  
632 pmid: 9284123.
- 633 20. Klima CL, Cook SR, Zaheer R, Laing C, Gannon VP, Xu Y, et al. Comparative  
634 genomic analysis of *Mannheimia haemolytica* from bovine sources. *PLoS One.* 2016; 11:  
635 e0149520. doi: 10.1371/journal.pone.0149520. pmid: 26926339.
- 636 21. Davies RL, Donachie W. Intra-specific diversity and host specificity within  
637 *Pasteurella haemolytica* based on variation of capsular polysaccharide, lipopolysaccharide  
638 and outer-membrane proteins. *Microbiology.* 1996; 142: 1895-907. doi:  
639 doi:10.1099/13500872-142-7-1895.
- 640 22. Lacroix RP, Duncan JR, Jenkins RP, Leitch RA, Perry JA, Richards JC. Structural  
641 and serological specificities of *Pasteurella haemolytica* lipopolysaccharides. *Infect Immun.*  
642 1993; 61: 170-81. pmid: 8418039.
- 643 23. Davies RL, Whittam TS, Selander RK. Sequence diversity and molecular evolution of  
644 the leukotoxin (*lktA*) gene in bovine and ovine strains of *Mannheimia (Pasteurella)*

- 645 *haemolytica*. J Bacteriol. 2001; 183: 1394-404. doi: 10.1128/jb.183.4.1394-1404.2001. pmid:  
646 11157953.
- 647 24. Davies RL, Lee I. Sequence diversity and molecular evolution of the heat-modifiable  
648 outer membrane protein gene (*ompA*) of *Mannheimia (Pasteurella) haemolytica*,  
649 *Mannheimia glucosida*, and *Pasteurella trehalosi*. J Bacteriol. 2004; 186: 5741-52. pmid:  
650 15317779.
- 651 25. Lee I, Davies RL. Evidence for a common gene pool and frequent recombinational  
652 exchange of the *tbpBA* operon in *Mannheimia haemolytica*, *Mannheimia glucosida* and  
653 *Bibersteinia trehalosi*. Microbiology. 2011; 157: 123-35. pmid: 20884693.
- 654 26. Ayalew S, Blackwood ER, Confer AW. Sequence diversity of the immunogenic outer  
655 membrane lipoprotein PlpE from *Mannheimia haemolytica* serotypes 1, 2, and 6. Vet  
656 Microbiol. 2006; 114: 260-8. doi: 10.1016/j.vetmic.2005.11.067. pmid: 16386856.
- 657 27. Grey CL, Thomson RG. *Pasteurella haemolytica* in the tracheal air of calves. Can J  
658 Comp Med. 1971; 35: 121-8. pmid: 4253460.
- 659 28. Lawrence PK, Nelson WR, Liu W, Knowles DP, Foreyt WJ, Srikumaran S. beta(2)  
660 integrin Mac-1 is a receptor for *Mannheimia haemolytica* leukotoxin on bovine and ovine  
661 leukocytes. Vet Immunol Immunopathol. 2008; 122: 285-94. doi:  
662 10.1016/j.vetimm.2007.12.005. pmid: 18262657.
- 663 29. Zecchinon L, Fett T, Desmecht D. How *Mannheimia haemolytica* defeats host  
664 defence through a kiss of death mechanism. Vet Res. 2005; 36: 133-56. doi:  
665 10.1051/vetres:2004065. pmid: 15720968.
- 666 30. Kisiela DI, Czuprynski CJ. Identification of *Mannheimia haemolytica* adhesins  
667 involved in binding to bovine bronchial epithelial cells. Infect Immun. 2009; 77: 446-55. doi:  
668 10.1128/IAI.00312-08. pmid: PMC2612293.

- 669 31. Lin C, Agnes JT, Behrens N, Shao M, Tagawa Y, Gershwin LJ, et al. *Histophilus*  
670 *somni* stimulates expression of antiviral proteins and inhibits BRSV replication in bovine  
671 respiratory epithelial cells. PLoS One. 2016; 11: e0148551. doi:  
672 10.1371/journal.pone.0148551. pmid: 26859677.
- 673 32. Rivera-Rivas JJ, Kisiela D, Czuprynski CJ. Bovine herpesvirus type 1 infection of  
674 bovine bronchial epithelial cells increases neutrophil adhesion and activation. Vet Immunol  
675 Immunopathol. 2009; 131: 167-76. doi: 10.1016/j.vetimm.2009.04.002. pmid: 19406483.
- 676 33. Abraham G, Zizzadoro C, Kacza J, Ellenberger C, Abs V, Franke J, et al. Growth and  
677 differentiation of primary and passaged equine bronchial epithelial cells under conventional  
678 and air-liquid-interface culture conditions. BMC Vet Res. 2011; 7: 26. doi: 10.1186/1746-  
679 6148-7-26. pmid: PMC3117700.
- 680 34. Balder R, Krunkosky TM, Nguyen CQ, Feezel L, Lafontaine ER. Hag mediates  
681 adherence of *Moraxella catarrhalis* to ciliated human airway cells. Infect Immun. 2009; 77:  
682 4597-608. doi: 10.1128/IAI.00212-09. pmid: PMC2747927.
- 683 35. Bateman AC, Karasin AI, Olsen CW. Differentiated swine airway epithelial cell  
684 cultures for the investigation of influenza A virus infection and replication. Influenza Other  
685 Respir Viruses. 2013; 7: 139-50. doi: 10.1111/j.1750-2659.2012.00371.x. pmid:  
686 PMC3443301.
- 687 36. Goris K, Uhlenbruck S, Schwegmann-Wessels C, Köhl W, Niedorf F, Stern M, et al.  
688 Differential sensitivity of differentiated epithelial cells to respiratory viruses reveals different  
689 viral strategies of host infection. J Virol. 2009; 83: 1962-8. doi: 10.1128/jvi.01271-08. pmid:  
690 19052091.
- 691 37. Kirchhoff J, Uhlenbruck S, Goris K, Keil GM, Herrler G. Three viruses of the bovine  
692 respiratory disease complex apply different strategies to initiate infection. Vet Res. 2014; 45:  
693 20. doi: 10.1186/1297-9716-45-20. pmid: 24548739.

- 694 38. Krunkosky TM, Jordan JL, Chambers E, Krause DC. *Mycoplasma pneumoniae* host-  
695 pathogen studies in an air-liquid culture of differentiated human airway epithelial cells.  
696 Microb Pathog. 2007; 42: 98-103. doi: 10.1016/j.micpath.2006.11.003. pmid: 17261358.
- 697 39. Lam E, Ramke M, Groos S, Warnecke G, Heim A. A differentiated porcine bronchial  
698 epithelial cell culture model for studying human adenovirus tropism and virulence. J Virol  
699 Methods. 2011; 78: 117-23. doi: 10.1016/j.jviromet.2011.08.025. pmid: 21907242.
- 700 40. Palermo LM, Porotto M, Yokoyama CC, Palmer SG, Mungall BA, Greengard O, et  
701 al. Human parainfluenza virus infection of the airway epithelium: viral hemagglutinin-  
702 neuraminidase regulates fusion protein activation and modulates infectivity. J Virol. 2009;  
703 83: 6900-8. doi: 10.1128/jvi.00475-09. pmid: 19386708.
- 704 41. Prince OA, Krunkosky TM, Krause DC. *In vitro* spatial and temporal analysis of  
705 *Mycoplasma pneumoniae* colonization of human airway epithelium. Infect Immun. 2014; 82:  
706 579-86. doi: 10.1128/IAI.01036-13. pmid: 24478073.
- 707 42. Schwab UE, Fulcher ML, Randell SH, Flaminio MJ, Russell DG. Equine bronchial  
708 epithelial cells differentiate into ciliated and mucus producing cells *in vitro*. In Vitro Cell Dev  
709 Biol Anim. 2010; 46: 102-6. doi: 10.1007/s11626-009-9258-6. pmid: 19915928.
- 710 43. Villenave R, Thavagnanam S, Sarlang S, Parker J, Douglas I, Skibinski G, et al. *In*  
711 *vitro* modeling of respiratory syncytial virus infection of pediatric bronchial epithelium, the  
712 primary target of infection in vivo. Proc Natl Acad Sci USA. 2012; 109. doi:  
713 10.1073/pnas.1110203109. pmid: 22411804.
- 714 44. Cozens D, Grahame E, Sutherland E, Taylor G, Berry C, Davies R. Development and  
715 optimization of a differentiated airway epithelial cell model of the bovine respiratory tract.  
716 Sci Rep. 2017; (submitted).

- 717 45. Cozens D, Sutherland E, Marchesi F, Taylor G, Berry CC, Davies RL. Temporal  
718 differentiation of bovine airway epithelial cells grown at an air-liquid interface. *J Histochem*  
719 *Cytochem.* 2017; (submitted).
- 720 46. Grumbach Y, Quynh NV, Chiron R, Urbach V. LXA4 stimulates ZO-1 expression  
721 and transepithelial electrical resistance in human airway epithelial (16HBE14o-) cells. *Am J*  
722 *Physiol Lung Cell Mol Physiol.* 2009; 296: L101-8. doi: 10.1152/ajplung.00018.2008. pmid:  
723 18849442.
- 724 47. Garcia-Medina R, Dunne WM, Singh PK, Brody SL. *Pseudomonas aeruginosa*  
725 acquires biofilm-like properties within airway epithelial cells. *Infect Immun.* 2005; 73: 8298-  
726 305. doi: 10.1128/IAI.73.12.8298-8305.2005. pmid: PMC1307054.
- 727 48. Bucior I, Pielage JF, Engel JN. *Pseudomonas aeruginosa* pili and flagella mediate  
728 distinct binding and signaling events at the apical and basolateral surface of airway  
729 epithelium. *PLoS Pathog.* 2012; 8: e1002616. doi: 10.1371/journal.ppat.1002616. pmid:  
730 22496644.
- 731 49. Halldorsson S, Gudjonsson T, Gottfredsson M, Singh PK, Gudmundsson GH,  
732 Baldursson O. Azithromycin maintains airway epithelial integrity during *Pseudomonas*  
733 *aeruginosa* infection. *Am J Respir Cell Mol Biol.* 2010; 42: 62-8. doi: 10.1165/rcmb.2008-  
734 0357OC. pmid: 19372247.
- 735 50. Ren D, Nelson KL, Uchakin PN, Smith AL, Gu X-X, Daines DA. Characterization of  
736 extended co-culture of non-typeable *Haemophilus influenzae* with primary human respiratory  
737 tissues. *Exp Biol Med.* 2012; 237: 540-7. doi: 10.1258/ebm.2012.011377.
- 738 51. Ketterer MR, Shao JQ, Hornick DB, Buscher B, Bandi VK, Apicella MA. Infection of  
739 primary human bronchial epithelial cells by *Haemophilus influenzae*: macropinocytosis as a  
740 mechanism of airway epithelial cell entry. *Infect Immun.* 1999; 67: 4161-70. pmid:  
741 10417188.

- 742 52. van Schilfgaarde M, van Alphen L, Eijk P, Everts V, Dankert J. Paracytosis of  
743 *Haemophilus influenzae* through cell layers of NCI-H292 lung epithelial cells. *Infect Immun.*  
744 1995; 63: 4729-37. pmid: 7591129.
- 745 53. Sutherland TC, Quattroni P, Exley RM, Tang CM. Transcellular passage of *Neisseria*  
746 *meningitidis* across a polarized respiratory epithelium. *Infect Immun.* 2010; 78: 3832-47. doi:  
747 10.1128/iai.01377-09. pmid: 20584970.
- 748 54. Galdiero M, Pisciotta MG, Marinelli A, Petrillo G, Galdiero E. Coinfection with  
749 BHV-1 modulates cell adhesion and invasion by *P. multocida* and *Mannheimia (Pasteurella)*  
750 *haemolytica*. *New Microbiol.* 2002; 25: 427-36. pmid: 12437222.
- 751 55. N'Jai A U, Rivera J, Atapattu DN, Owusu-Ofori K, Czuprynski CJ. Gene expression  
752 profiling of bovine bronchial epithelial cells exposed *in vitro* to bovine herpesvirus 1 and  
753 *Mannheimia haemolytica*. *Vet Immunol Immunopathol.* 2013; 155: 182-9. doi:  
754 10.1016/j.vetimm.2013.06.012. pmid: 23890750.
- 755 56. Boukahil I, Czuprynski CJ. *Mannheimia haemolytica* biofilm formation on bovine  
756 respiratory epithelial cells. *Vet Microbiol.* 2016; 197: 129-36. doi:  
757 10.1016/j.vetmic.2016.11.012. pmid: 27938674.
- 758 57. Ostrowski LE, Nettekheim P. Inhibition of ciliated cell differentiation by fluid  
759 submersion. *Exp Lung Res.* 1995; 21: 957-70. pmid: 8591796.
- 760 58. Griffith LG, Swartz MA. Capturing complex 3D tissue physiology *in vitro*. *Nat Rev*  
761 *Mol Cell Biol.* 2006; 7: 211-24. doi: 10.1038/nrm1858. pmid: 16496023.
- 762 59. Ma Y, Han F, Liang J, Yang J, Shi J, Xue J, et al. A species-specific activation of  
763 Toll-like receptor signaling in bovine and sheep bronchial epithelial cells triggered by  
764 Mycobacterial infections. *Mol Immunol.* 2016; 71: 23-33. doi:  
765 10.1016/j.molimm.2016.01.004. pmid: 26802731.



- 766 60. Highlander SK. Molecular genetic analysis of virulence in *Mannheimia (Pasteurella)*  
767 *haemolytica*. Front Biosci. 2001; 6: D1128-50. pmid: 11532607.
- 768 61. Frank GH, Smith PC. Prevalence of *Pasteurella haemolytica* in transported calves.  
769 Am J Vet Res. 1983; 44: 981-5. pmid: 6870030.
- 770 62. Haig S-J. Adherence of *Mannheimia haemolytica* to ovine bronchial epithelial cells.  
771 Biosci Horiz. 2011; 4: 50-60. doi: 10.1093/biohorizons/hzr007.
- 772 63. Clark AB, Randell SH, Nettesheim P, Gray TE, Bagnell B, Ostrowski LE. Regulation  
773 of ciliated cell differentiation in cultures of rat tracheal epithelial cells. Am J Respir Cell Mol  
774 Biol. 1995; 12: 329-38. doi: 10.1165/ajrcmb.12.3.7873199. pmid: 7873199.
- 775 64. Spassky N, Meunier A. The development and functions of multiciliated epithelia. Nat  
776 Rev Mol Cell Biol. 2017. doi: 10.1038/nrm.2017.21. pmid: 28400610.
- 777 65. Taha-Abdelaziz K, Wyer L, Berghuis L, Bassel LL, Clark ME, Caswell JL.  
778 Regulation of tracheal antimicrobial peptide gene expression in airway epithelial cells of  
779 cattle. Vet Res. 2016; 47: 44. doi: 10.1186/s13567-016-0329-x.
- 780 66. Diamond G, Russell JP, Bevins CL. Inducible expression of an antibiotic peptide gene  
781 in lipopolysaccharide-challenged tracheal epithelial cells. Proc Natl Acad Sci U S A. 1996;  
782 93: 5156-60.
- 783 67. Mitchell GB, Al-Haddawi MH, Clark ME, Beveridge JD, Caswell JL. Effect of  
784 corticosteroids and neuropeptides on the expression of defensins in bovine tracheal epithelial  
785 cells. Infect Immun. 2007; 75. doi: 10.1128/IAI.00686-06.
- 786 68. Taha-Abdelaziz K, Perez-Casal J, Schott C, Hsiao J, Attah-Poku S, Slavic D, et al.  
787 Bactericidal activity of tracheal antimicrobial peptide against respiratory pathogens of cattle.  
788 Vet Immunol Immunopathol. 2013; 152. doi: 10.1016/j.vetimm.2012.12.016.

- 789 69. Coburn J, Frank DW. Macrophages and Epithelial Cells Respond Differently to the  
790 *Pseudomonas aeruginosa* Type III Secretion System. *Infect Immun.* 1999; 67: 3151-4. pmid:  
791 PMC96636.
- 792 70. Cano V, Moranta D, Llobet-Brossa E, Bengoechea JA, Garmendia J. *Klebsiella*  
793 *pneumoniae* triggers a cytotoxic effect on airway epithelial cells. *BMC Microbiol.* 2009; 9:  
794 156. doi: 10.1186/1471-2180-9-156. pmid: 19650888.
- 795 71. McClenahan D, Hellenbrand K, Atapattu D, Aulik N, Carlton D, Kapur A, et al.  
796 Effects of Lipopolysaccharide and *Mannheimia haemolytica* Leukotoxin on Bovine Lung  
797 Microvascular Endothelial Cells and Alveolar Epithelial Cells. *Clin Vaccine Immunol.* 2008;  
798 15: 338-47. doi: 10.1128/CVI.00344-07. pmid: PMC2238055.
- 799 72. Kim M, Ashida H, Ogawa M, Yoshikawa Y, Mimuro H, Sasakawa C. Bacterial  
800 Interactions with the Host Epithelium. *Cell Host Microbe.* 2010; 8: 20-35. doi:  
801 <https://doi.org/10.1016/j.chom.2010.06.006>.
- 802 73. Ribet D, Cossart P. How bacterial pathogens colonize their hosts and invade deeper  
803 tissues. *Microbes Infect.* 2015; 17: 173-83. doi: <https://doi.org/10.1016/j.micinf.2015.01.004>.
- 804 74. Bals R, Hiemstra PS. Innate immunity in the lung: how epithelial cells fight against  
805 respiratory pathogens. *Eur Respir J.* 2004; 23: 327-33. doi: 10.1183/09031936.03.00098803.  
806 pmid: 14979512.
- 807 75. Ganesan S, Comstock AT, Sajjan US. Barrier function of airway tract epithelium.  
808 *Tissue Barriers.* 2013; 1: e24997. doi: 10.4161/tisb.24997. pmid: 24665407.
- 809 76. Plotkowski MC, de Bentzmann S, Pereira SH, Zahm JM, Bajolet-Laudinat O, Roger  
810 P, et al. *Pseudomonas aeruginosa* internalization by human epithelial respiratory cells  
811 depends on cell differentiation, polarity, and junctional complex integrity. *Am J Respir Cell*  
812 *Mol Biol.* 1999; 20: 880-90. doi: 10.1165/ajrcmb.20.5.3408. pmid: 10226058.

813 77. Kim JY, Sajjan US, Krasan GP, LiPuma JJ. Disruption of tight junctions during  
814 traversal of the respiratory epithelium by *Burkholderia cenocepacia*. *Infect Immun*. 2005; 73:  
815 7107-12. doi: 10.1128/iai.73.11.7107-7112.2005. pmid: 16239504.

816 78. Higgins G, Fustero Torre C, Tyrrell J, McNally P, Harvey BJ, Urbach V. Lipoxin A4  
817 prevents tight junction disruption and delays the colonization of cystic fibrosis bronchial  
818 epithelial cells by *Pseudomonas aeruginosa*. *Am J Physiol Lung Cell Mol Physiol*. 2016;  
819 310: L1053.

820

821 **Figure 1. Infection of undifferentiated BBEC cultures by *M. haemolytica* strains.** BBEC  
822 cultures were infected apically with *M. haemolytica* strains PH2 or PH202 ( $2.5 \times 10^7$   
823 cfu/insert) at day 0 post-ALI. At 0.5, 1, 2 and 24 hpi, cultures were apically washed to  
824 remove unbound bacteria, and colonisation assessed. (A) Quantification of the number of (i)  
825 adherent *M. haemolytica* and (ii) *M. haemolytica* present in the apical wash, as expressed as a  
826 percentage of the original inoculum. Three inserts were analysed per time point, and the data  
827 represents the mean +/- standard deviation from cultures derived from three different animals.  
828 (B-C) Cultures were fixed at the stated time post-infection and immunostained to detect  
829 colonisation of *M. haemolytica* with (B)  $\beta$ -tubulin (*M. haemolytica* - green;  $\beta$ -tubulin - red;  
830 nuclei - blue; x1000 magnification) or (C) tight junctions (*M. haemolytica* - green; ZO-1 -  
831 red; nuclei - blue; x1000 magnification). Representative images are shown of *M.*  
832 *haemolytica* strains (i) PH2 or (ii) PH202 at 2 and 24 hpi (see Fig S1 and S2).

833 **Figure 2. Differentiated BBEC cultures replicate the bovine bronchial epithelium.**  
834 BBEC cultures were grown for 21 days at an ALI before fixation; sample of *ex vivo* tissue  
835 were also taken from the donor animal. Morphology was subsequently assessed using (A)  
836 examination by SEM (x2500 magnification) and (B) H&E stained histological sections  
837 (x1000 magnification). Representative images are shown of (i) *ex vivo* bovine bronchial  
838 epithelium and (ii) uninfected differentiated BBECs 21 days post-ALI. (C) BBEC cultures  
839 21 days post-ALI were immunostained for markers of differentiation. Representative images  
840 are shown displaying (i) cilia formation ( $\beta$ -tubulin - red; nuclei - blue; x1000 magnification)  
841 and (ii) tight junction formation (ZO-1 - red; nuclei - blue; x1000 magnification).

842 **Figure 3. Adhesion of PH2 and PH202 to differentiated BBEC cultures.** BBEC cultures  
843 were infected apically with *M. haemolytica* strains PH2 or PH202 ( $2.5 \times 10^7$  cfu/insert) at day  
844 21 post-ALI. At stated time points post-infection, cultures were apically washed to remove  
845 unbound bacteria. Quantification of the number of (A) adherent *M. haemolytica* and (B) *M.*

846 *haemolytica* present in the apical wash per insert, as expressed as a percentage of the original  
847 inoculum. Three inserts were analysed per time point, and the data represents the mean +/-  
848 standard deviation.

849 **Figure 4. Infection of differentiated BBEC cultures by *M. haemolytica* PH2.** BBEC  
850 cultures were infected apically with *M. haemolytica* strain PH2 ( $2.5 \times 10^7$  cfu/insert) at day 21  
851 post-ALI. At stated time points post-infection, cultures were apically washed to remove  
852 unbound bacteria, and fixed. Colonisation of PH2 was subsequently assessed using (A)  
853 immunofluorescence labelling of PH2 and cilia (*M. haemolytica* - green;  $\beta$ -tubulin - red;  
854 nuclei – blue; x1000 magnification), (B) examination by SEM (x2500 magnification) and (C)  
855 immunohistochemical-labelling of PH2 in histological sections (OmpA-labelled *M.*  
856 *haemolytica* stained brown; x1000 magnification). Representative images are shown of  
857 BBEC cultures at (i) 6, (ii) 12, (iii) 16, (iv) 20 and (v) 24 hpi (see Fig S3, S4 and S5).

858 **Figure 5. Infection of differentiated BBEC cultures by *M. haemolytica* PH202.** BBEC  
859 cultures were infected apically with *M. haemolytica* strain PH202 ( $2.5 \times 10^7$  cfu/insert) at day  
860 21 post-ALI. At stated time points post-infection, cultures were apically washed to remove  
861 unbound bacteria, and fixed. Colonisation of PH202 was subsequently assessed using (A)  
862 immunofluorescence labelling of PH202 and cilia (*M. haemolytica* - green;  $\beta$ -tubulin - red;  
863 nuclei – blue; x1000 magnification), (B) examination by SEM (x2500 magnification) and (C)  
864 immunohistochemical-labelling of PH202 in histological sections (OmpA-labelled *M.*  
865 *haemolytica* stained brown; x1000 magnification). Representative images are shown of  
866 BBEC cultures at (i) 6, (ii) 12, (iii) 16, (iv) 20 and (v) 24 hpi (see Fig S3, S4 and S5).

867 **Figure 6. Histological assessment of *M. haemolytica* infection of differentiated BBEC**  
868 **cultures.** BBEC cultures were infected apically with *M. haemolytica* strains (A) PH2 or (B)  
869 PH202 ( $2.5 \times 10^7$  cfu/insert) at day 21 post-ALI. At stated time points post-infection, cultures

870 were apically washed to remove unbound bacteria, fixed and paraffin-embedded using  
871 standard histological techniques. Sections were subsequently cut, deparaffinised and H&E  
872 stained. Representative images are shown of BBEC cultures at (i) 6, (ii) 12, (iii) 16, (iv) 20  
873 and (v) 24 hpi (x1000 magnification; see Fig S6).

874 **Figure 7. Internalisation of *M. haemolytica* in differentiated BBEC cultures.** BBEC  
875 cultures were infected apically with *M. haemolytica* strains PH2 or PH202 ( $2.5 \times 10^7$   
876 cfu/insert) at day 21 post-ALI. At 24 hpi, cultures were apically washed to remove unbound  
877 bacteria. (A) The number of intracellular bacteria was quantified using a gentamicin  
878 protection assay, expressed as a percentage of the original inoculum. Three inserts were  
879 analysed per condition, and the data represents the mean +/- standard deviation. (B-C) BBEC  
880 cultures infected with PH2 (24 hpi) were assessed using microscopy. (B) Z-stack orthogonal  
881 representation of a BBEC culture labelled for PH2 and cilia (*M. haemolytica* - green;  $\beta$ -  
882 tubulin - red; nuclei – blue; x630 magnification). (C) Examination by SEM. Representative  
883 images shown of (i) invasion of a non-ciliated epithelial cell by PH2 (x10000 magnification)  
884 and (ii) an epithelial cell with apical membrane removed displaying intracellular PH2 (x5000  
885 magnification).

886 **Figure 8. Tight junction integrity in differentiated BBEC cultures following *M.***  
887 ***haemolytica* infection.** BBEC cultures were infected apically with *M. haemolytica* strains  
888 PH2 or PH202 ( $2.5 \times 10^7$  cfu/insert) at day 21 post-ALI. At stated time points post-infection,  
889 cultures were apically washed to remove unbound bacteria. Colonisation and tight junction  
890 integrity was subsequently assessed using (A) labelling of *M. haemolytica* and ZO-1 (*M.*  
891 *haemolytica* - green; ZO-1 - red; nuclei – blue; x1000 magnification). Representative images  
892 are shown of BBEC cultures at (i) 6, (ii) 12, (iii) 16, (iv) 20 and (v) 24 hpi (see Fig S7). (B)  
893 Tight-junction integrity of BBEC cultures apically infected with *M. haemolytica* was also  
894 assessed by measuring the TEER at the stated time points post-infection. (C) BBEC cultures

895 were treated for 18 h with differing concentrations of lipoxin A4 to stabilise tight junctions  
896 prior to apical infection with *M. haemolytica* strain PH2 ( $2.5 \times 10^7$  cfu/insert) at day 21 post-  
897 ALI. At 24 hpi, cultures were apically washed to remove unbound bacteria, and the number  
898 of adherent *M. haemolytica* quantified and expressed as a percentage of the original  
899 inoculum. For all of the above quantifications, three inserts were analysed per condition, and  
900 the data represents the mean +/- standard deviation.

901 **Figure 9. Quantification of adhesion of *M. haemolytica* strains to differentiated BBEC**  
902 **cultures.** BBEC cultures were infected apically with eight strains of *M. haemolytica* ( $2.5 \times$   
903  $10^7$  cfu/insert) at day 21 post-ALI. (A) At stated time points post-infection, cultures were  
904 apically washed to remove unbound bacteria, and colonisation assessed. Quantification of (i)  
905 the number of adherent *M. haemolytica* and (ii) *M. haemolytica* present in the apical wash, as  
906 expressed as a percentage of the original inoculum. (B) Tight-junction integrity of BBEC  
907 cultures apically infected with eight strains *M. haemolytica* was also assessed by measuring  
908 the TEER at the stated time points post-infection. For all of the above quantifications, three  
909 inserts were analysed per condition, and the data represents the mean +/- standard deviation  
910 from cultures derived from three different animals (see Fig S8).

911 **Figure 10. Colonisation of *M. haemolytica* strains to differentiated BBEC cultures.**  
912 BBEC cultures were infected apically with eight strains of *M. haemolytica* ( $2.5 \times 10^7$   
913 cfu/insert) at day 21 post-ALI. At 24 hpi, cultures were apically washed to remove unbound  
914 bacteria, and fixed. Colonisation of *M. haemolytica* was subsequently assessed using (A)  
915 immunohistochemical-labelling of *M. haemolytica* in histological sections (OmpA-labelled  
916 *M. haemolytica* stained brown; x1000 magnification) and (B) examination by SEM (x2500  
917 magnification). Representative images are shown of BBEC cultures infected with (i) PH2,  
918 (ii) PH376, (iii) PH202, (iv) PH210, (v) PH278, (vi) PH376, (vii) PH62 and (viii) PH346 (see  
919 Fig S9, S10 and S11).

920 **Table 1. *M. haemolytica* strains utilised in this investigation.**

921 **Table 2. Assessment of damage to the differentiated BBEC cultures following PH2 and**

922 **PH202 infection.** BBEC cultures were infected apically with *M. haemolytica* strains PH2 or

923 PH202 ( $2.5 \times 10^7$  cfu/insert) at day 21 post-ALI. At stated time points post-infection cultures

924 were apically washed to remove unbound bacteria, fixed and paraffin-embedded using

925 standard histological techniques. Sections were subsequently cut, deparaffinised and H&E

926 stained. Semi-quantitative assessment of the extent of bacterial colonisation and epithelial

927 integrity in the histological sections was made visually. -, no sign of infection; +, low level

928 of infection, few foci of infection present; ++, moderate level of infection, foci of infection

929 common across the entirety of the culture; +++, high level of infection, infection present

930 across the majority of the culture not confined to foci, cell layer showed high levels of

931 degradation.

932 **Table 3. Assessment of damage to the differentiated BBEC cultures following *M.***

933 ***haemolytica* infection.** BBEC cultures were infected apically with eight strains of *M.*

934 *haemolytica* ( $2.5 \times 10^7$  cfu/insert) at day 21 post-ALI. At stated time points post-infection

935 cultures were apically washed to remove unbound bacteria, fixed and paraffin-embedded

936 using standard histological techniques. Sections were subsequently cut, deparaffinised and

937 H&E stained (see Fig S12). Semi-quantitative assessment of the extent of bacterial

938 colonisation and epithelial integrity in the histological sections was made visually. -, no sign

939 of infection; +, low level of infection, few foci of infection present; ++, moderate level of

940 infection, foci of infection common across the entirety of the culture; +++, high level of

941 infection, infection present across the majority of the culture not confined to foci, cell layer

942 showed high levels of degradation.

943



944 **Supplementary Figure 1. Immunofluorescent-labelling of *M. haemolytica* and  $\beta$ -tubulin**  
945 **following infection of undifferentiated BBEC cultures.** BBEC cultures were infected  
946 apically with *M. haemolytica* strains PH2 or PH202 ( $2.5 \times 10^7$  cfu/insert) at day 0 post-ALI.  
947 At 0.5, 1, 2 and 24 hpi, cultures were apically washed to remove unbound bacteria, and fixed.  
948 Colonisation of PH2 and PH202 was subsequently assessed using immunofluorescence  
949 labelling of *M. haemolytica* and  $\beta$ -tubulin (*M. haemolytica* - green;  $\beta$ -tubulin - red; nuclei –  
950 blue; x1000 magnification).

951 **Supplementary Figure 2. Immunofluorescent-labelling of *M. haemolytica* and ZO-1**  
952 **following infection of undifferentiated BBEC cultures.** BBEC cultures were infected  
953 apically with *M. haemolytica* strains PH2 or PH202 ( $2.5 \times 10^7$  cfu/insert) at day 0 post-ALI.  
954 At 0.5, 1, 2 and 24 hpi, cultures were apically washed to remove unbound bacteria, and fixed.  
955 Colonisation of PH2 and PH202 was subsequently assessed using immunofluorescence  
956 labelling of *M. haemolytica* and tight junctions (*M. haemolytica* - green; ZO-1 - red; nuclei –  
957 blue; x1000 magnification).

958 **Supplementary Figure 3. Immunofluorescent-labelling of PH2 or PH202 and  $\beta$ -tubulin**  
959 **following infection of differentiated BBEC cultures.** BBEC cultures were infected apically  
960 with *M. haemolytica* strains PH2 or PH202 ( $2.5 \times 10^7$  cfu/insert) at day 21 post-ALI. At  
961 stated time points post-infection, cultures were apically washed to remove unbound bacteria,  
962 and fixed. Colonisation of PH2 and PH202 was subsequently assessed using  
963 immunofluorescence labelling of *M. haemolytica* and cilia (*M. haemolytica* - green;  $\beta$ -tubulin  
964 - red; nuclei – blue; x1000 magnification).

965 **Supplementary Figure 4. SEM examination of PH2 or PH202 infection of differentiated**  
966 **BBEC cultures.** BBEC cultures were infected apically with *M. haemolytica* strains PH2 or  
967 PH202 ( $2.5 \times 10^7$  cfu/insert) at day 21 post-ALI. At stated time points post-infection, cultures

968 were apically washed to remove unbound bacteria, fixed and examination by SEM (x2500  
969 magnification).

970 **Supplementary Figure 5. Immunohistochemical-labelling of PH2 or PH202 in**  
971 **histological sections following infection of differentiated BBEC cultures.** BBEC cultures  
972 were infected apically with *M. haemolytica* strains PH2 or PH202 ( $2.5 \times 10^7$  cfu/insert) at day  
973 21 post-ALI. At stated time points post-infection, cultures were apically washed to remove  
974 unbound bacteria, fixed and paraffin-embedded using standard histological techniques.  
975 Sections were subsequently cut, deparaffinised and immunohistochemistry labelling of *M.*  
976 *haemolytica* was performed using an anti-OmpA antibody (OmpA-labelled *M. haemolytica*  
977 stained brown; x1000 magnification). For PH2 120 hpi, the tissue layer was too damaged to  
978 recover following antigen retrieval.

979 **Supplementary Figure 6. H&E staining of histological sections following PH2 or PH202**  
980 **infection of differentiated BBEC cultures.** BBEC cultures were infected apically with *M.*  
981 *haemolytica* strains PH2 or PH202 ( $2.5 \times 10^7$  cfu/insert) at day 21 post-ALI. At stated time  
982 points post-infection, cultures were apically washed to remove unbound bacteria, fixed and  
983 paraffin-embedded using standard histological techniques. Sections were subsequently cut,  
984 deparaffinised and H&E staining was performed (x1000 magnification).

985 **Supplementary Figure 7. Immunofluorescent-labelling of PH2 or PH202 and ZO-1**  
986 **following infection of differentiated BBEC cultures.** BBEC cultures were infected apically  
987 with *M. haemolytica* strains PH2 or PH202 ( $2.5 \times 10^7$  cfu/insert) at day 21 post-ALI. At  
988 stated time points post-infection, cultures were apically washed to remove unbound bacteria,  
989 and fixed. Colonisation of PH2 and PH202 and tight junction integrity was subsequently  
990 assessed using immunofluorescence labelling of *M. haemolytica* and tight junctions (*M.*  
991 *haemolytica* - green; ZO-1 - red; nuclei – blue; x1000 magnification).

992 **Supplementary Figure 8. Quantification of adhesion of *M. haemolytica* strains to**  
993 **differentiated BBEC cultures.** BBEC cultures were infected apically with eight strains of  
994 *M. haemolytica* ( $2.5 \times 10^7$  cfu/insert) at day 21 post-ALI. At 2, 24 or 72 hpi, cultures were  
995 apically washed to remove unbound bacteria, and colonisation assessed. Quantification of  
996 (A) the number of adherent *M. haemolytica* and (B) *M. haemolytica* present in the apical  
997 wash, as expressed as a percentage of the original inoculum. Three inserts were analysed per  
998 time point, and the data represents the mean +/- standard deviation.

999 **Supplementary Figure 9. Immunohistochemical-labelling of *M. haemolytica* strains in**  
1000 **histological sections following infection of differentiated BBEC cultures.** BBEC cultures  
1001 were infected apically with eight strains of *M. haemolytica* ( $2.5 \times 10^7$  cfu/insert) at day 21  
1002 post-ALI. At 2, 24 or 72 hpi, cultures were apically washed to remove unbound bacteria,  
1003 fixed and paraffin-embedded using standard histological techniques. Sections were  
1004 subsequently cut, deparaffinised and immunohistochemistry labelling of *M. haemolytica* was  
1005 performed using an anti-OmpA antibody (OmpA-labelled *M. haemolytica* stained brown;  
1006 x1000 magnification).

1007 **Supplementary Figure 10. SEM examination of differentiated BBEC culture infected**  
1008 **with bovine *M. haemolytica* isolates.** BBEC cultures were infected apically with *M.*  
1009 *haemolytica* strains PH2, PH376, PH202 or PH210 ( $2.5 \times 10^7$  cfu/insert) at day 21 post-ALI.  
1010 At 2, 24 or 72 hpi, cultures were apically washed to remove unbound bacteria, fixed and  
1011 examination by SEM (x2500 magnification).

1012 **Supplementary Figure 11. SEM examination of differentiated BBEC culture infected**  
1013 **with ovine *M. haemolytica* isolates.** BBEC cultures were infected apically with *M.*  
1014 *haemolytica* strains PH278, PH372, PH62 or PH346 ( $2.5 \times 10^7$  cfu/insert) at day 21 post-ALI.

1015 At 2, 24 or 72 hpi, cultures were apically washed to remove unbound bacteria, fixed and  
1016 examination by SEM (x2500 magnification).

1017 **Supplementary Figure 12. H&E staining of histological sections following *M.***

1018 ***haemolytica* infection of differentiated BBEC cultures.** BBEC cultures were infected  
1019 apically with eight strains of *M. haemolytica* ( $2.5 \times 10^7$  cfu/insert) at day 21 post-ALI. At 2,  
1020 24 or 72 hpi, cultures were apically washed to remove unbound bacteria, fixed and paraffin-  
1021 embedded using standard histological techniques. Sections were subsequently cut,  
1022 deparaffinised and H&E staining was performed (x1000 magnification).

## Figure 1

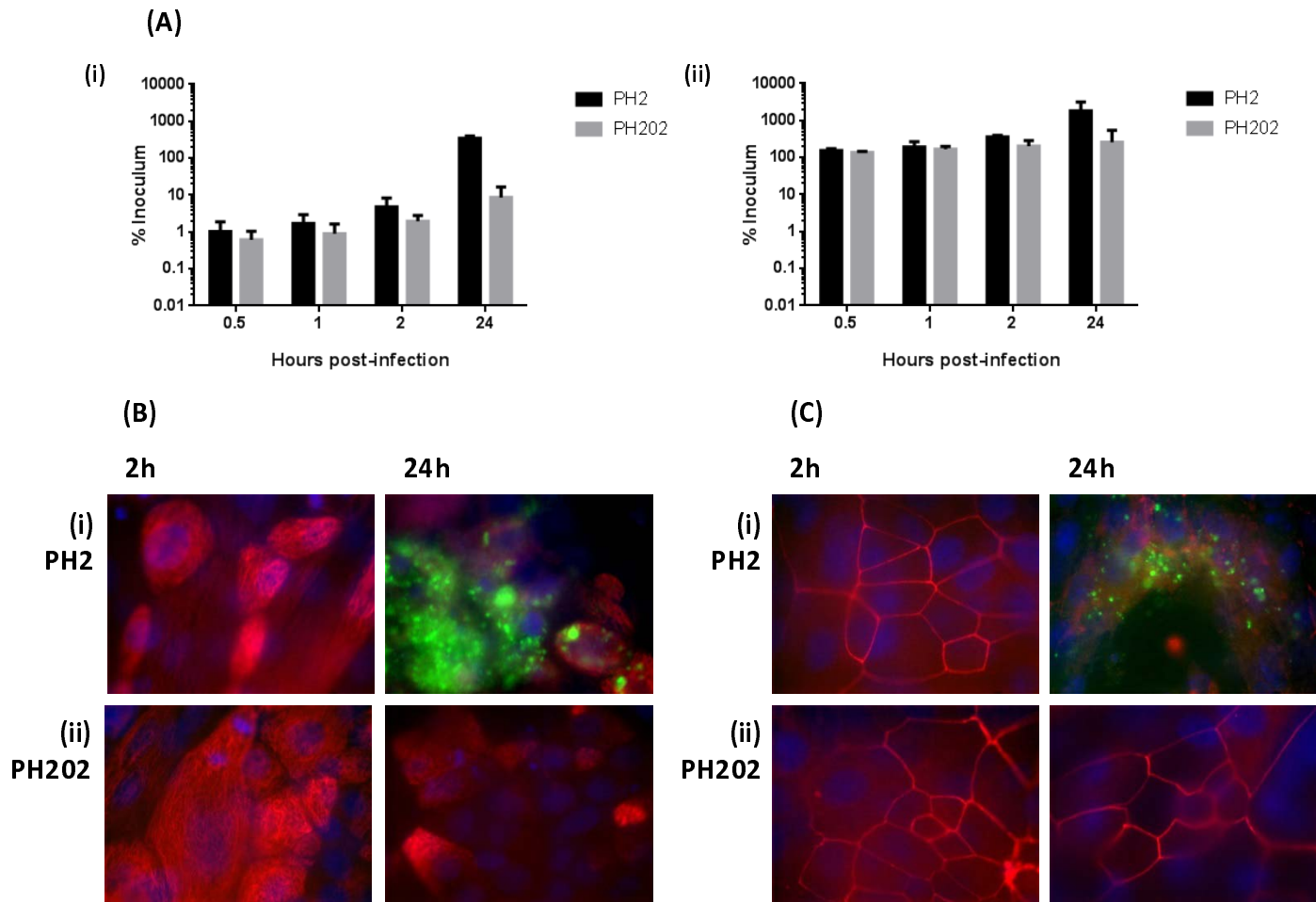


## Figure 2

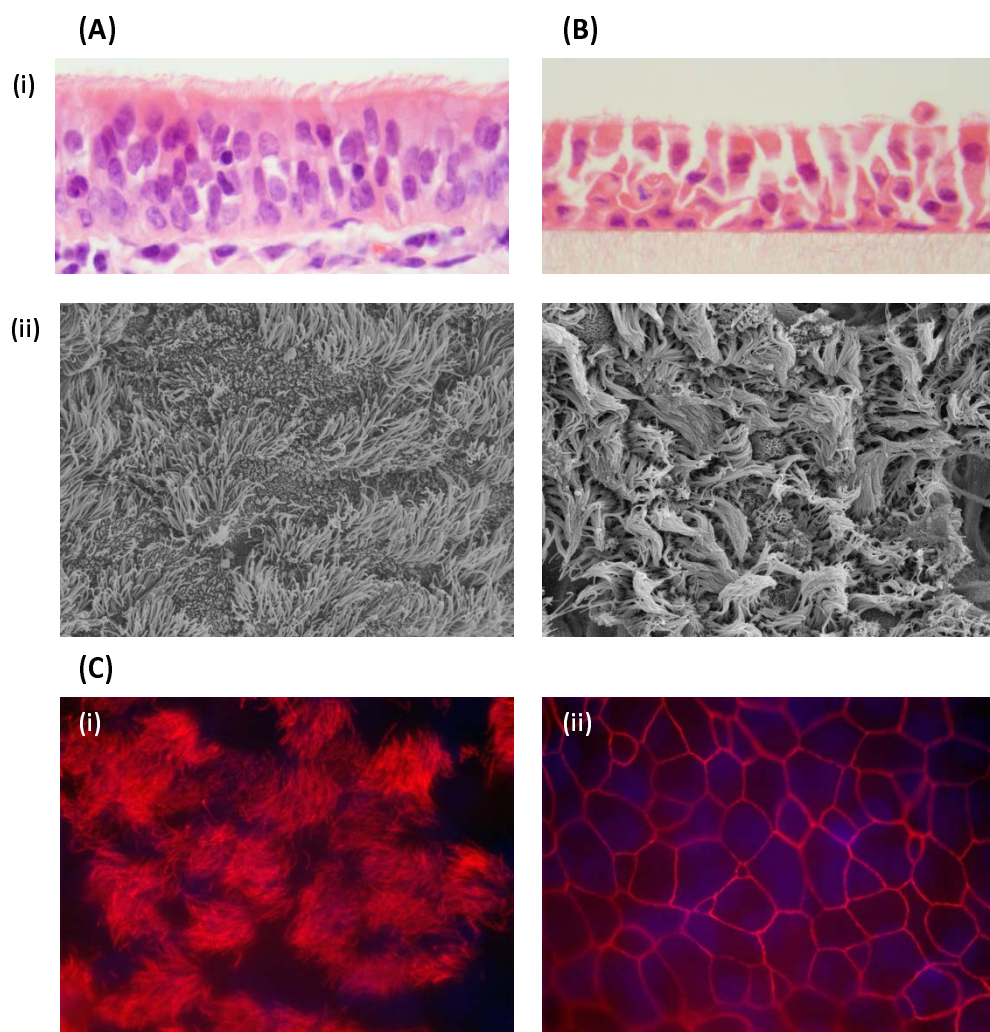


**Figure 3**

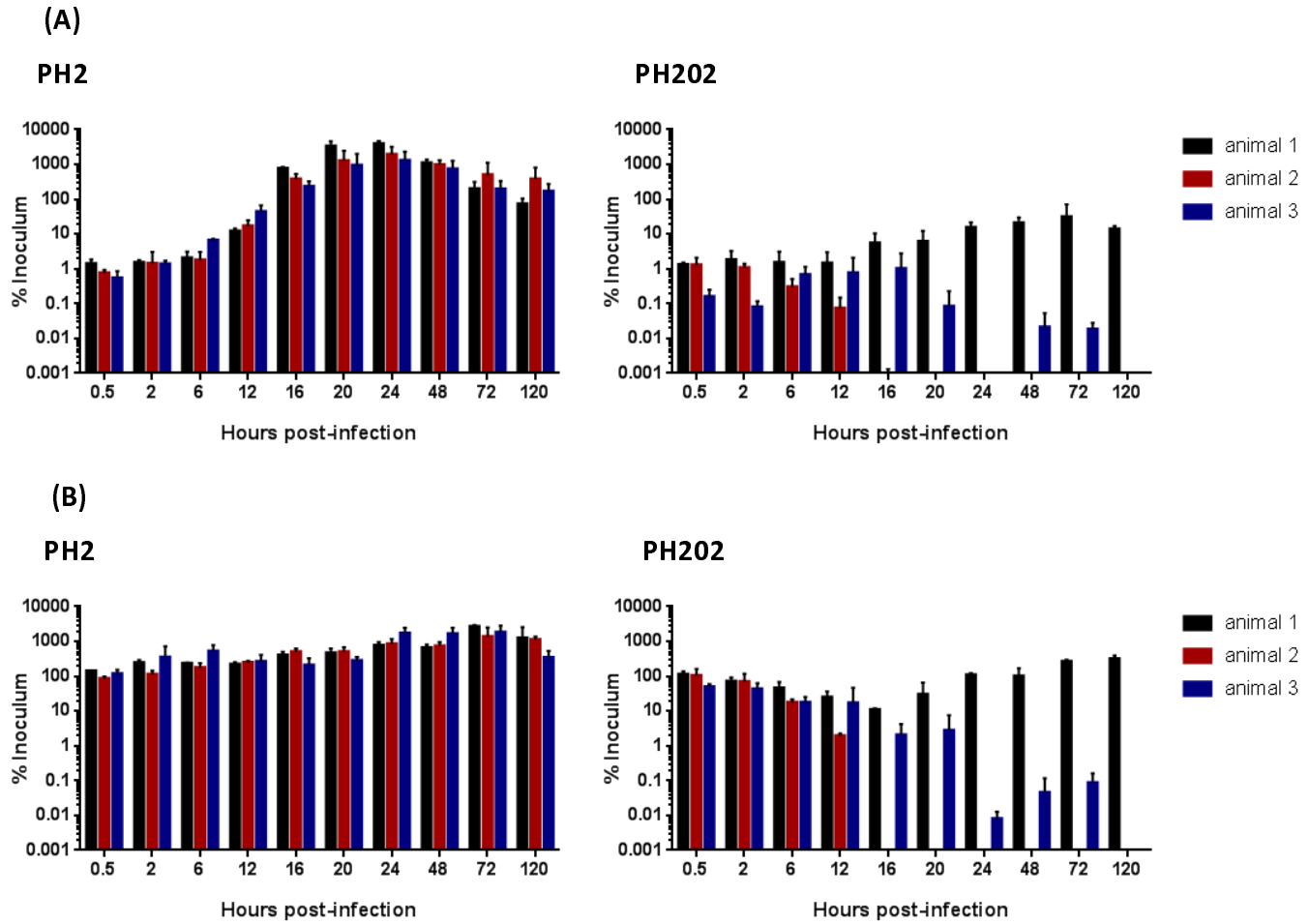


**Figure 4**

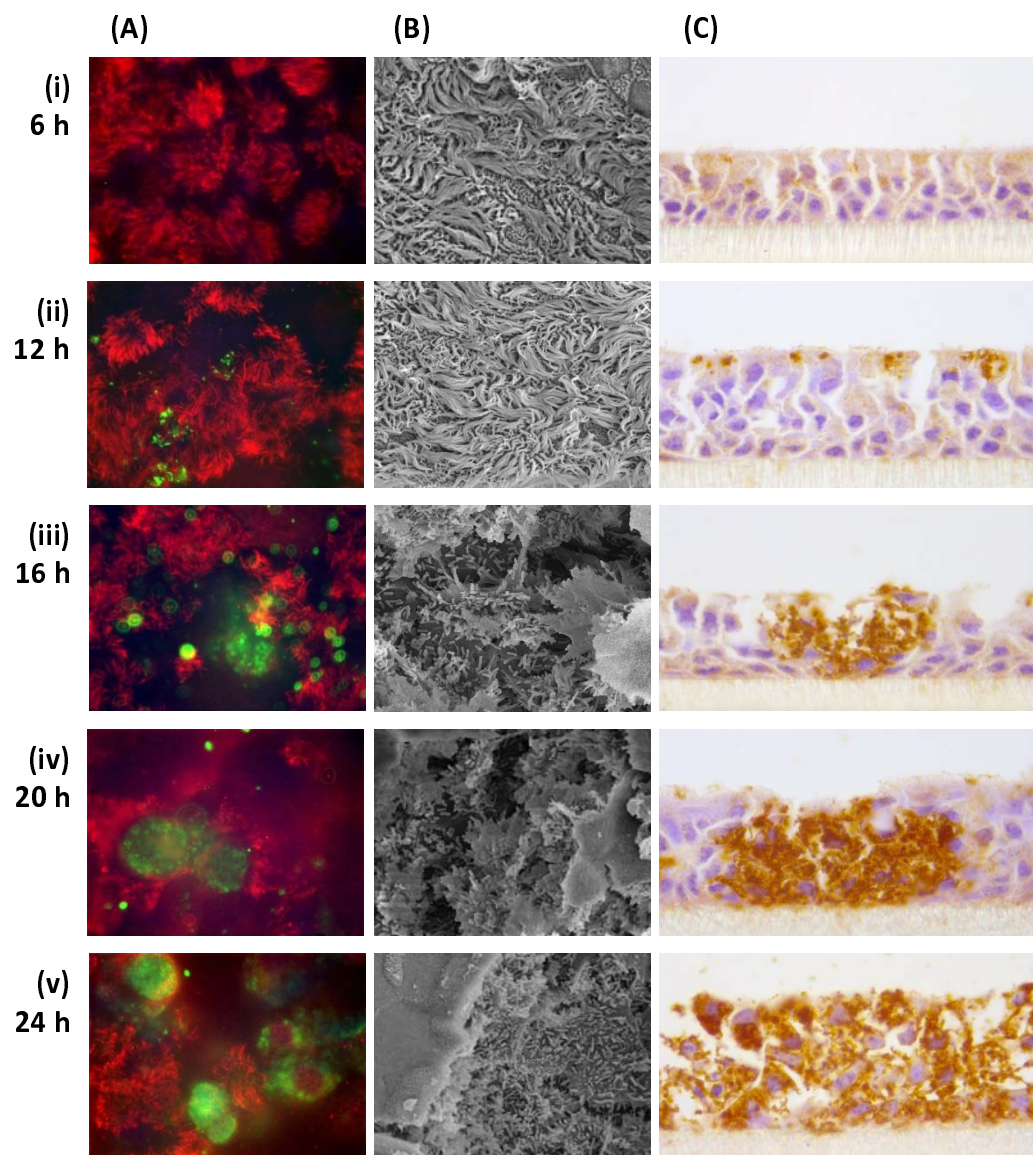




**Figure 5**

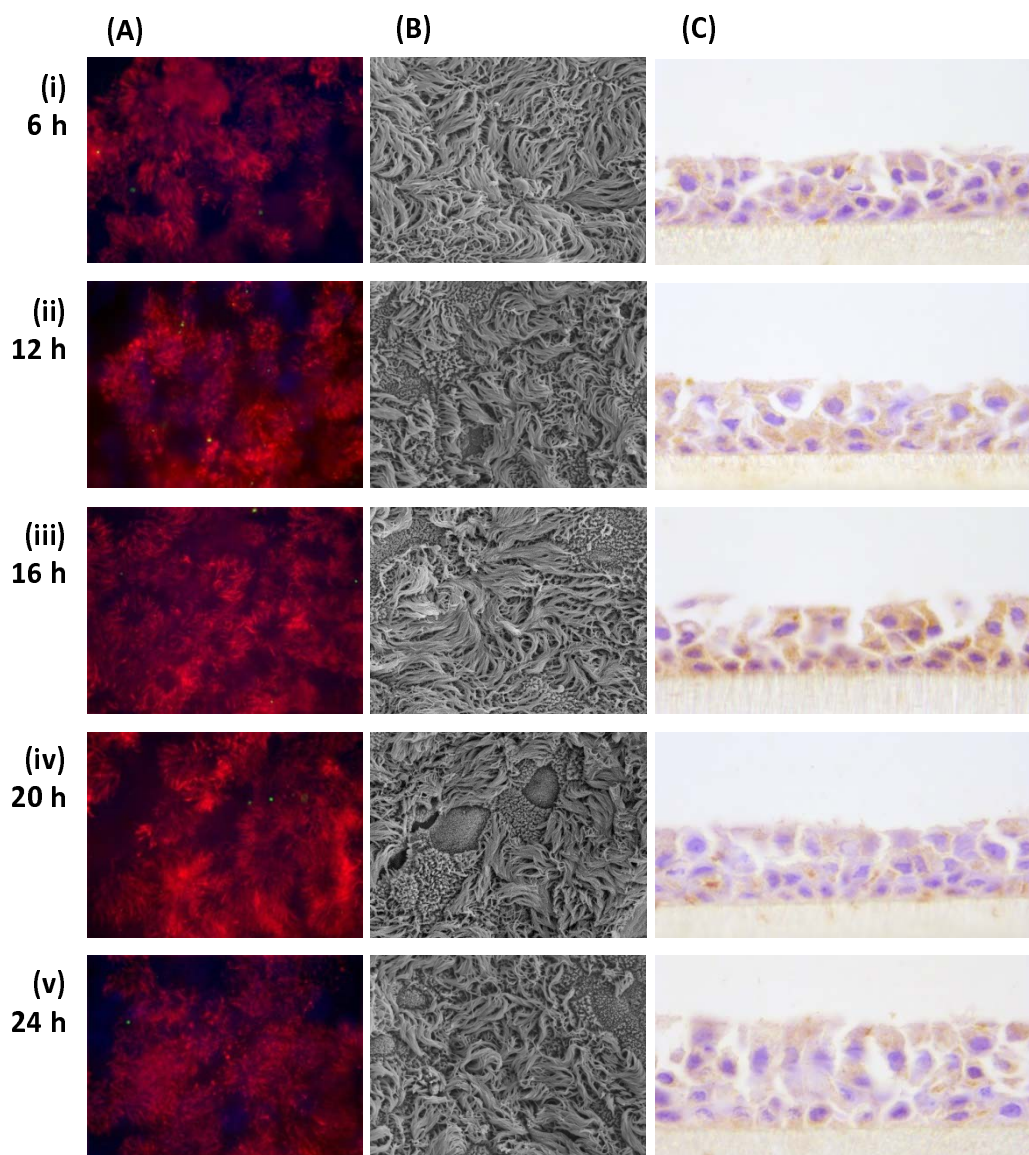


**Figure 6**

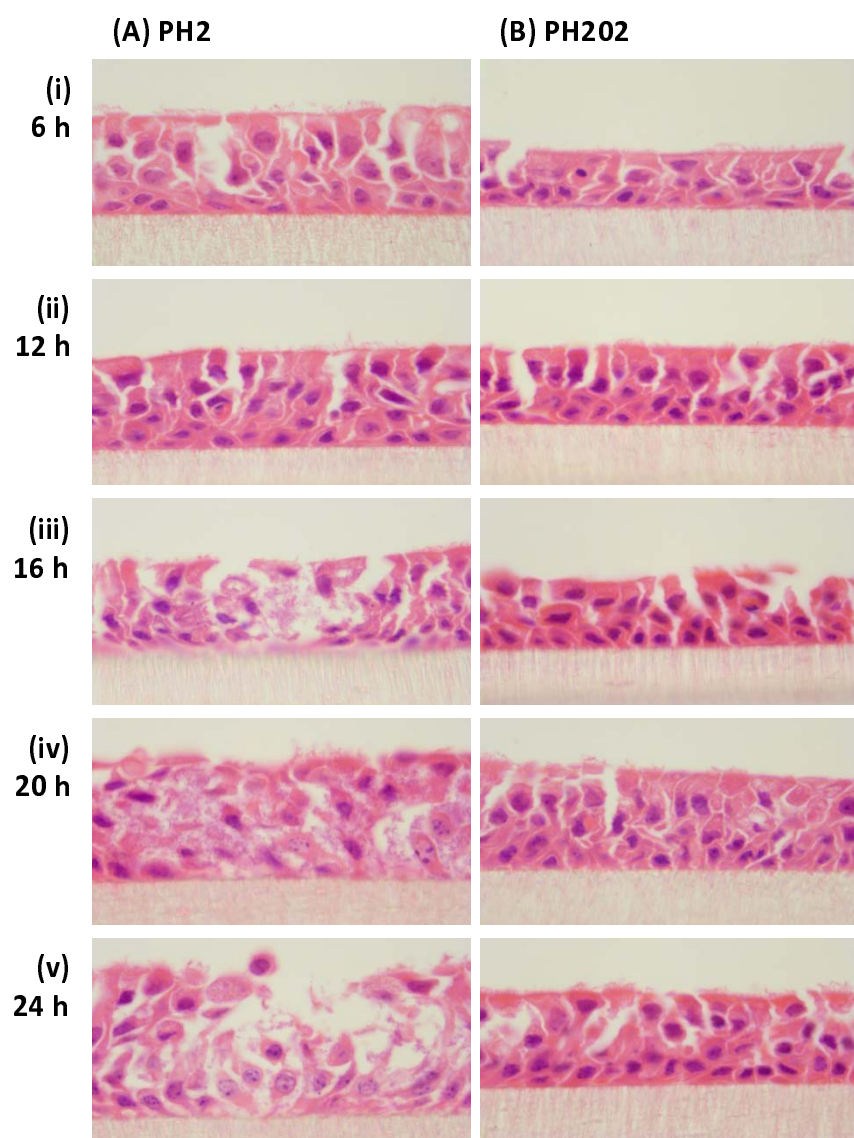


## Figure 7

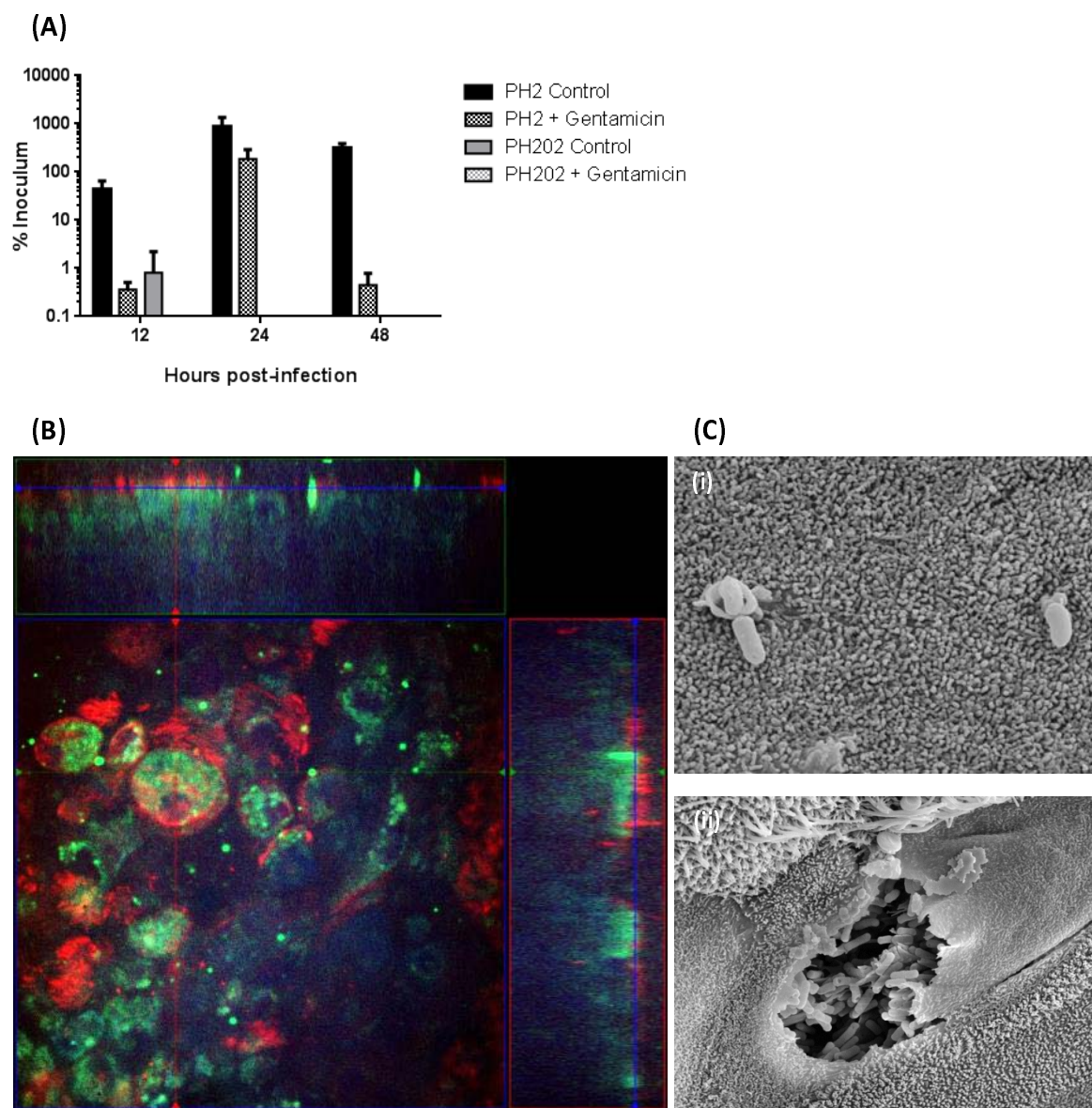


## Figure 8

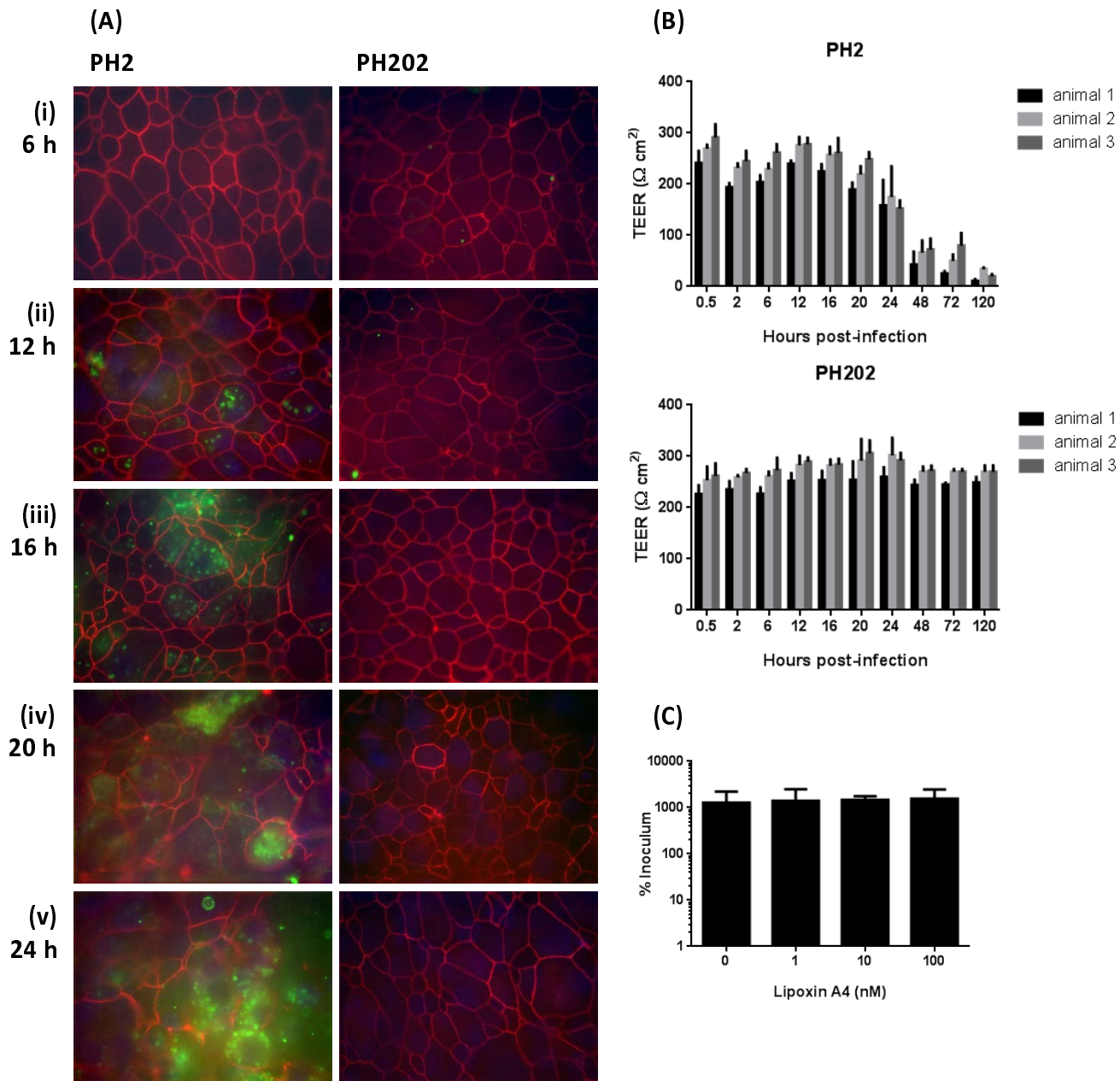


**Figure 9**

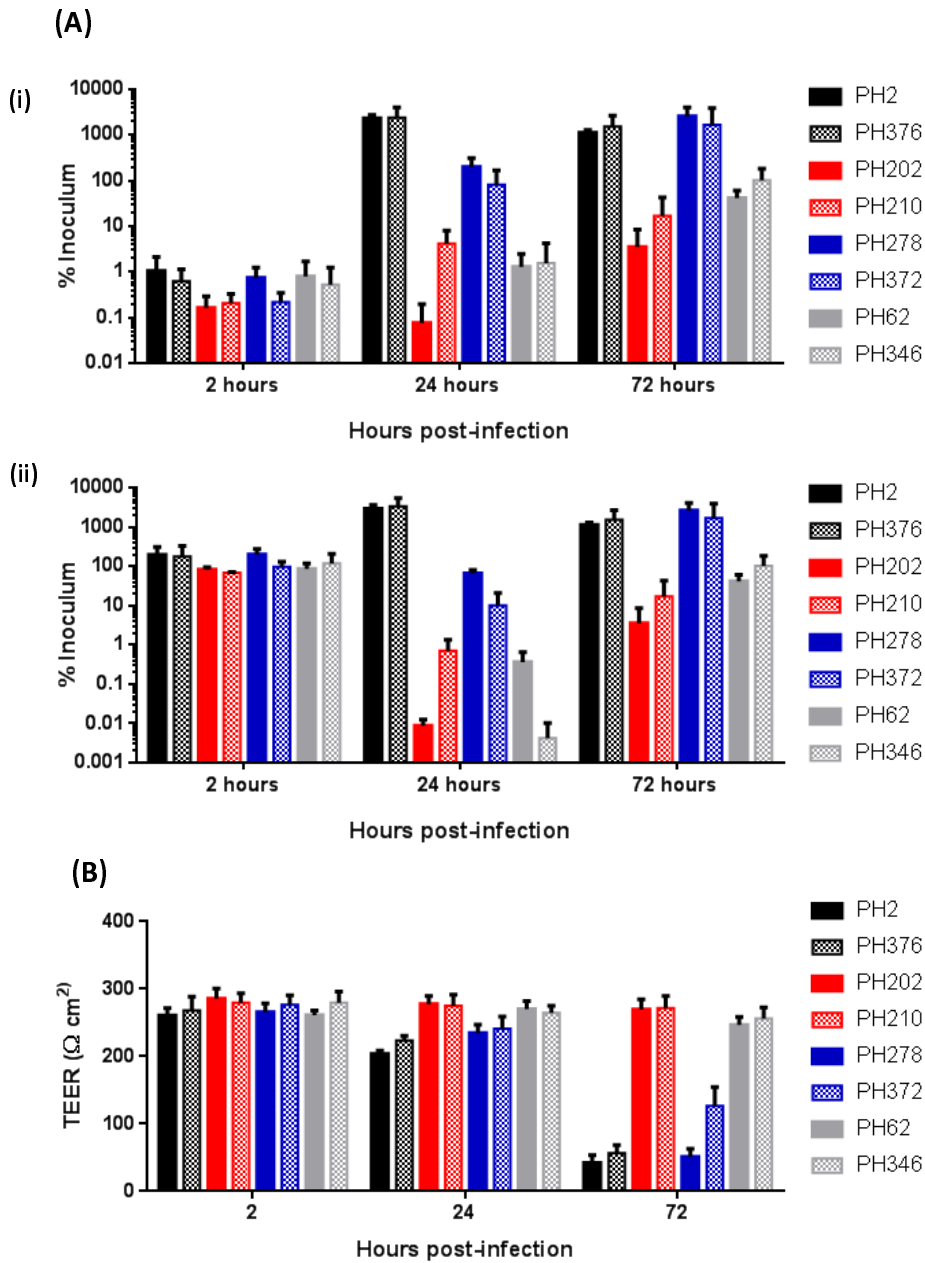


**Figure 10**

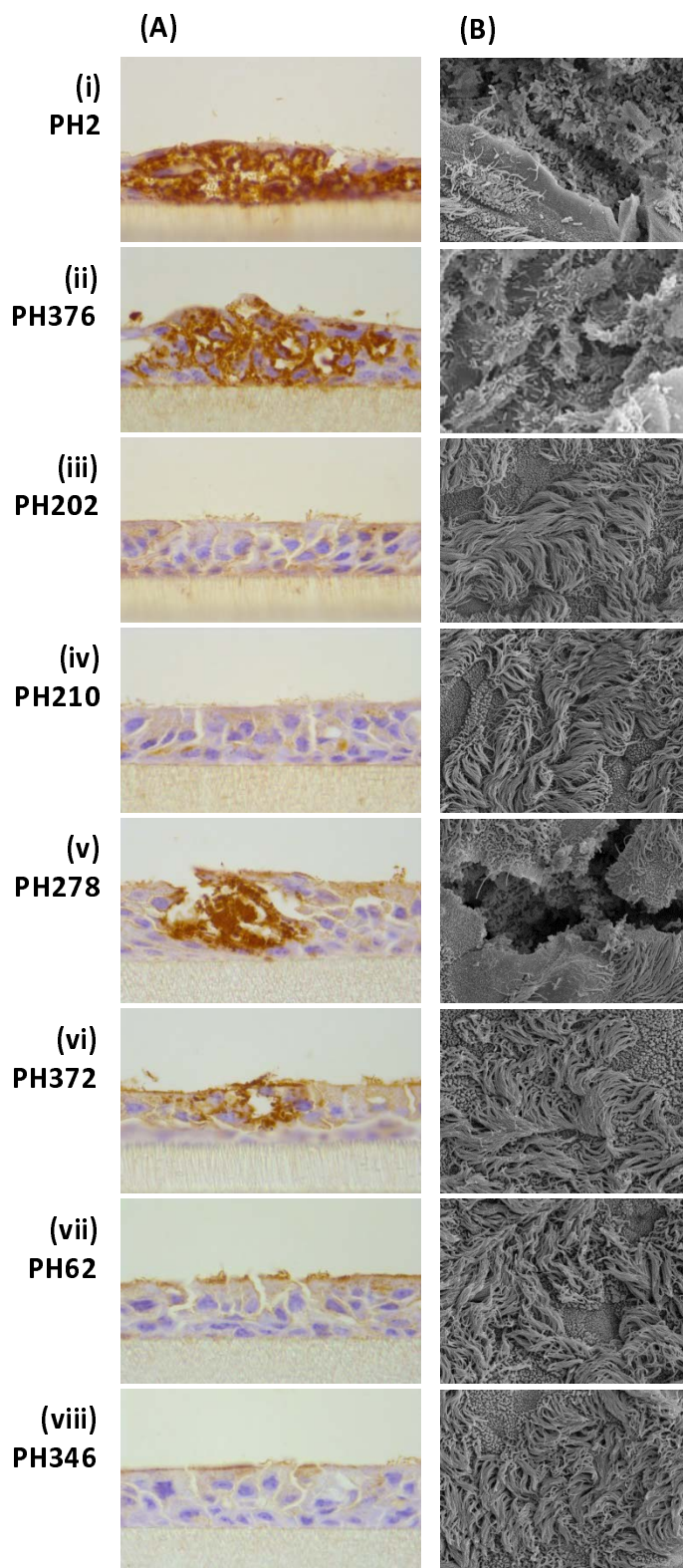


**Table 1**

<b>Isolate</b>	<b>Serotype</b>	<b>Host species</b>	<b>Clinical status</b>	<b>Site of Origin</b>
<b>PH2</b>	A1	Bovine	Pneumonia	Lung
<b>PH376</b>	A6	Bovine	Pneumonia	Lung
<b>PH202</b>	A2	Bovine	Healthy	Nasopharynx
<b>PH210</b>	A2	Bovine	Healthy	Nasopharynx
<b>PH278</b>	A2	Ovine	Pneumonia	Lung
<b>PH372</b>	A2	Ovine	Pneumonia	Lung
<b>PH62</b>	A12	Ovine	Healthy	Nasopharynx
<b>PH346</b>	A12	Ovine	Healthy	Nasopharynx

**Table 2**

Strain	PH2			PH202		
	Animal 1	Animal 2	Animal 3	Animal 1	Animal 2	Animal 3
<b>0.5h</b>	-	-	-	-	-	-
<b>2h</b>	-	-	-	-	-	-
<b>6h</b>	-	-	-	-	-	-
<b>12h</b>	+	+	-	-	-	-
<b>16h</b>	++	++	++	-	-	-
<b>20h</b>	++	++	++	-	-	-
<b>24h</b>	++	++	++	-	-	-
<b>48h</b>	+++	+++	+++	-	-	-
<b>72h</b>	+++	+++	+++	-	-	-
<b>120h</b>	+++	+++	+++	+++	-	-

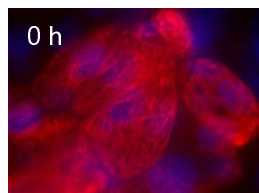


**Table 3**

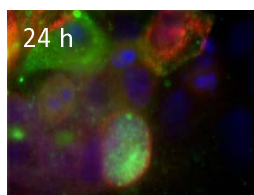
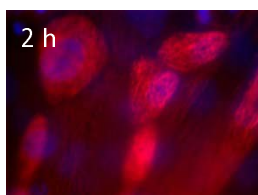
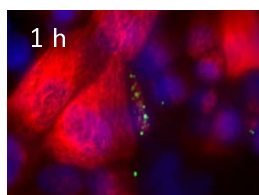
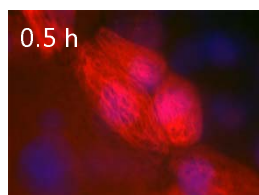
Strain	2 hours			24 hours			72 hours		
	Animal 1	Animal 2	Animal 3	Animal 1	Animal 2	Animal 3	Animal 1	Animal 2	Animal 3
PH2	-	-	-	++	++	++	+++	+++	+++
PH376	-	-	-	++	++	++	+++	+++	+++
PH202	-	-	-	-	-	-	-	-	-
PH210	-	-	-	+	-	-	-	-	-
PH278	-	-	-	++	++	+	+++	+++	++
PH372	-	-	-	+	+	+	++	+	++
PH62	-	-	-	-	+	-	+	-	-
PH346	-	-	-	+	+	-	-	-	-

## Supplementary Figure 1

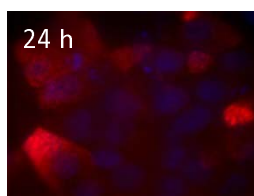
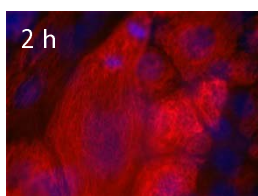
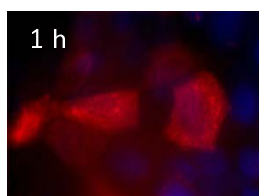
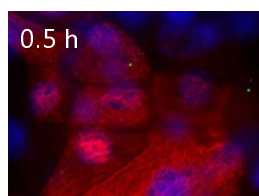
### Uninfected



### PH2

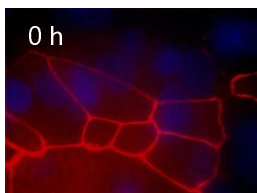


### PH202

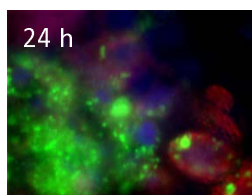
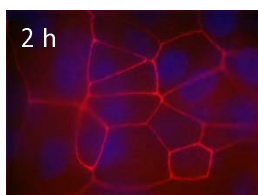
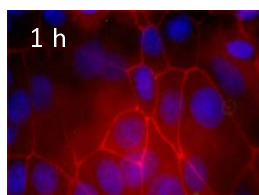
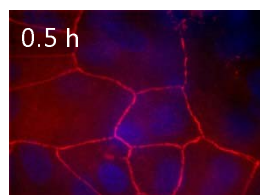


## Supplementary Figure 2

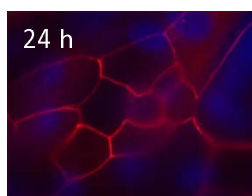
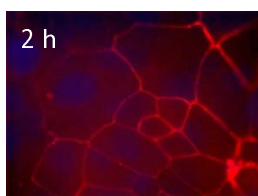
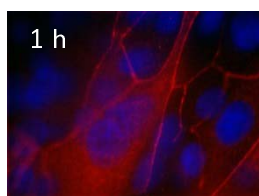
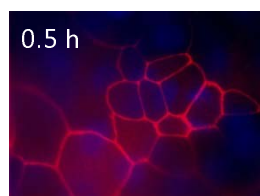
### Uninfected



### PH2

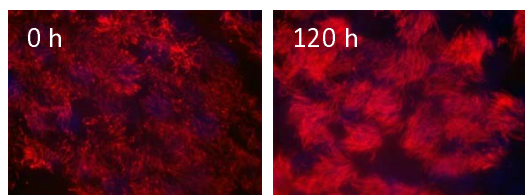


### PH202

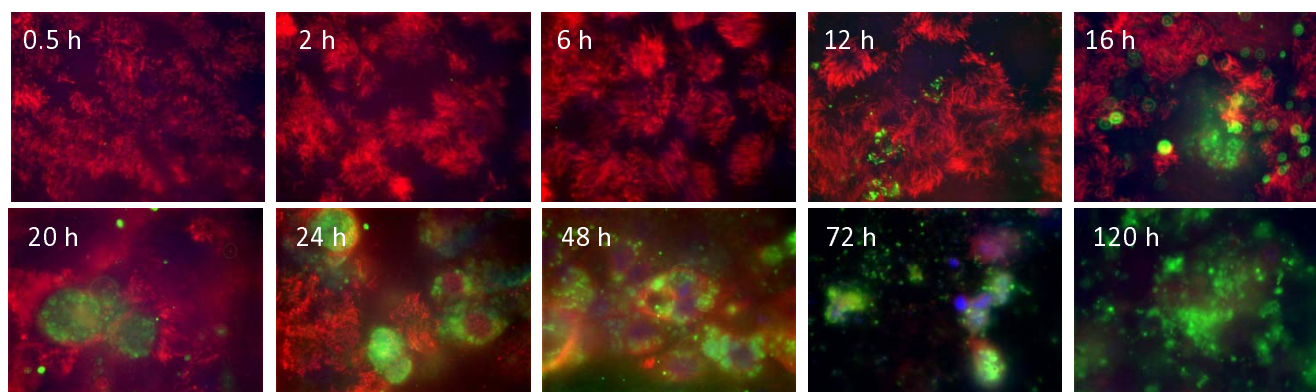


## Supplementary Figure 3

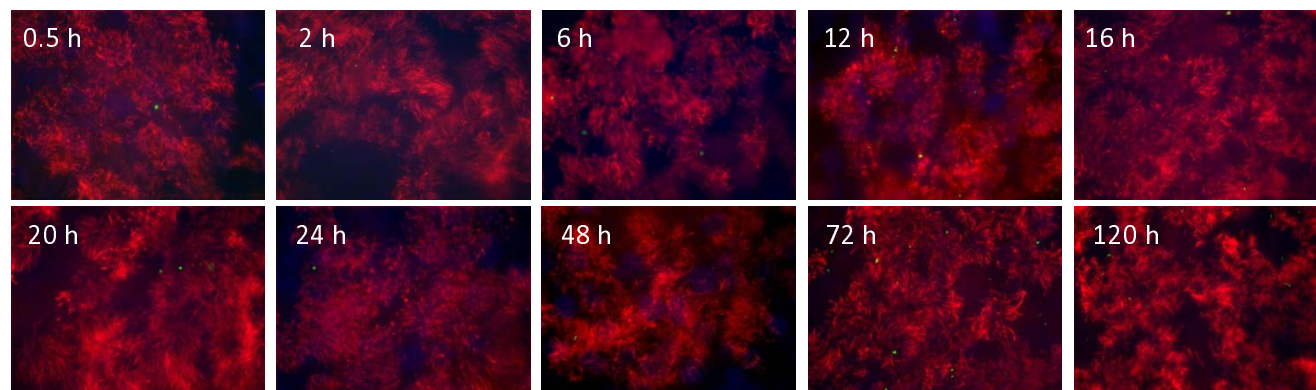
### Uninfected



### PH2

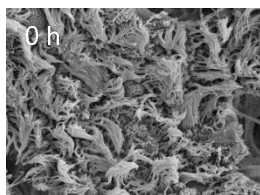


### PH202

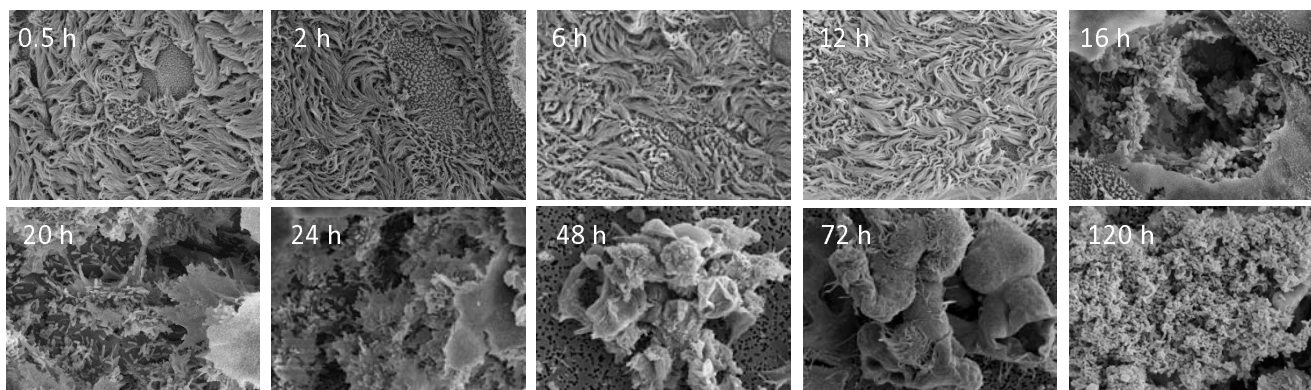


## Supplementary Figure 4

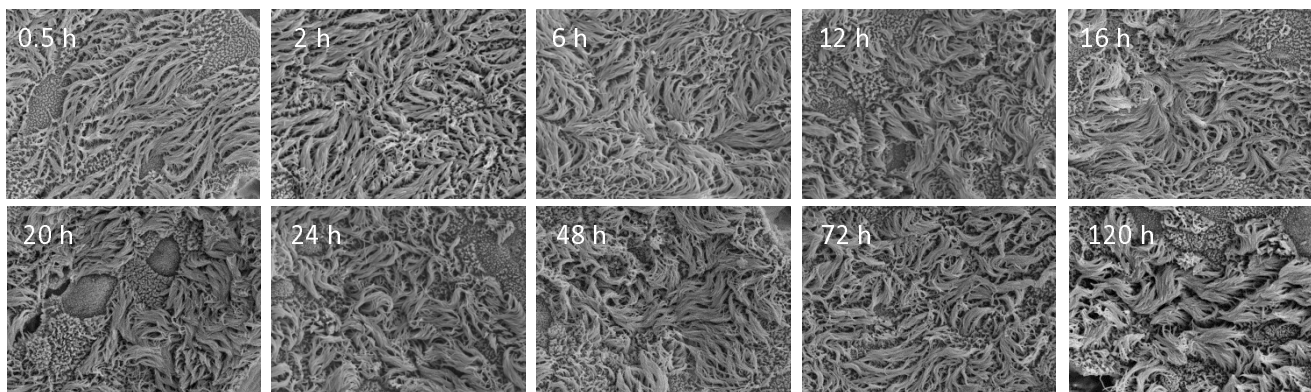
### Uninfected



### PH2

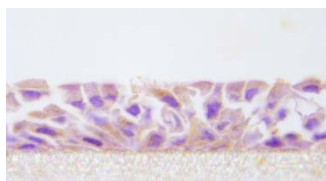


### PH202

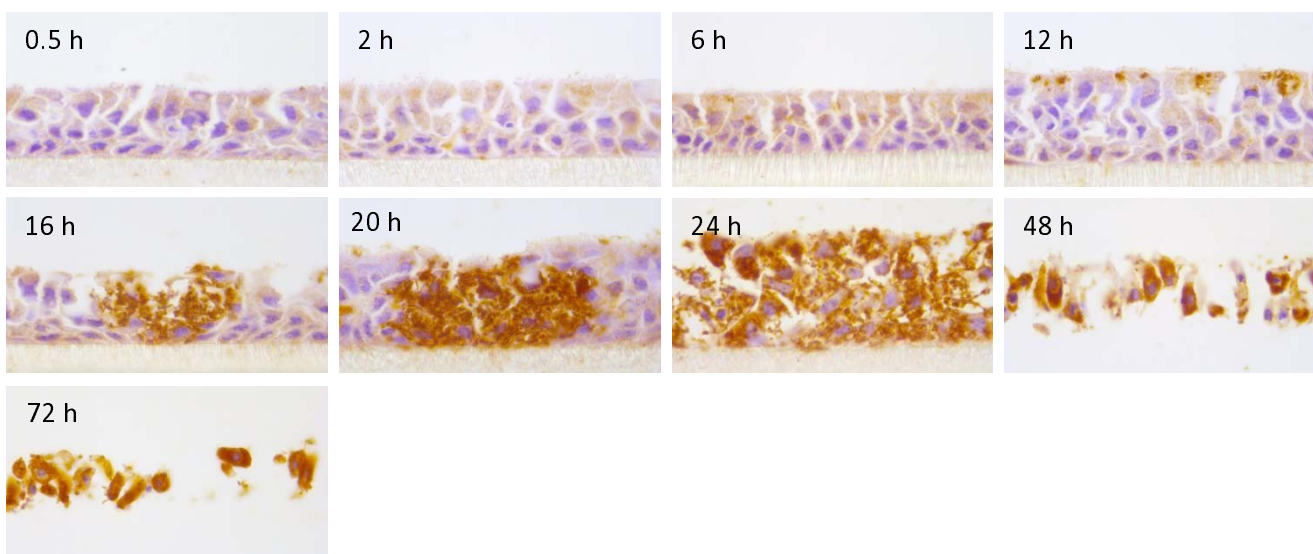


## Supplementary Figure 5

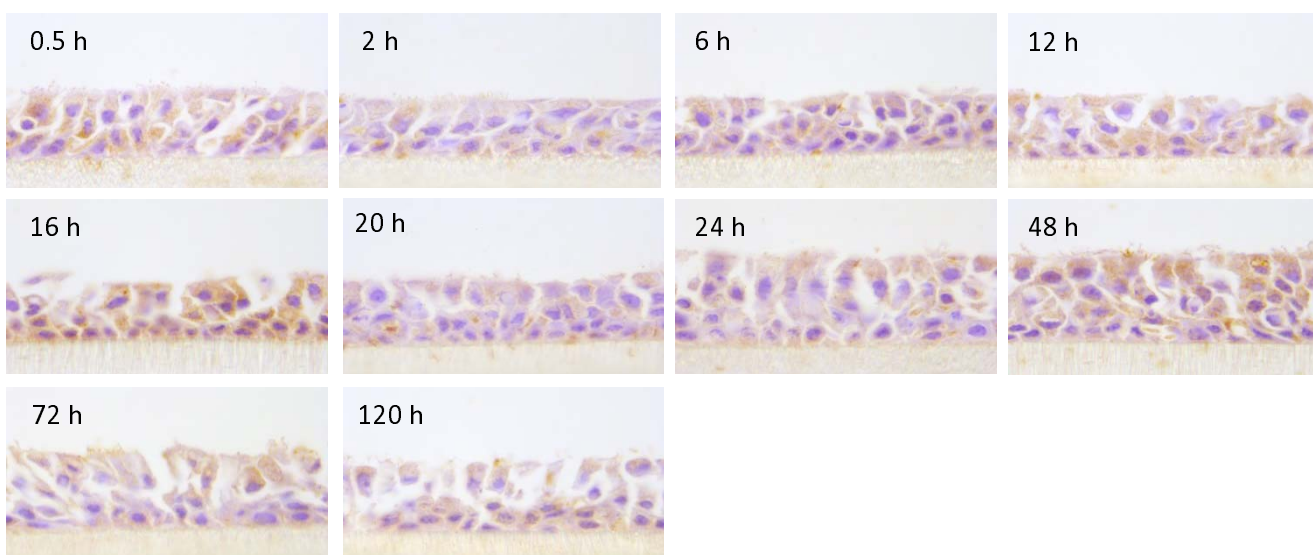
### Uninfected



### PH2

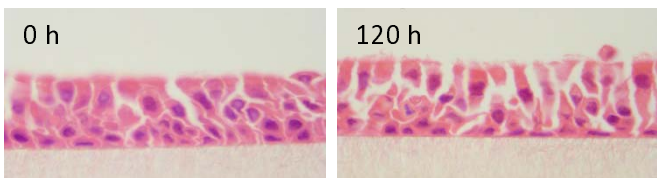


### PH202

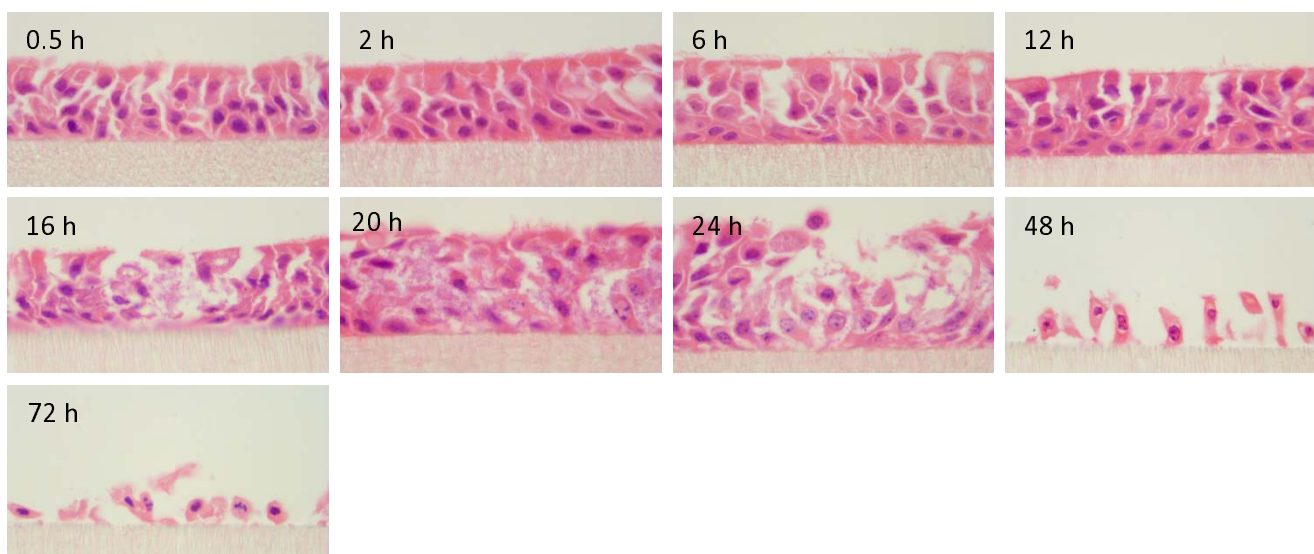


## Supplementary Figure 6

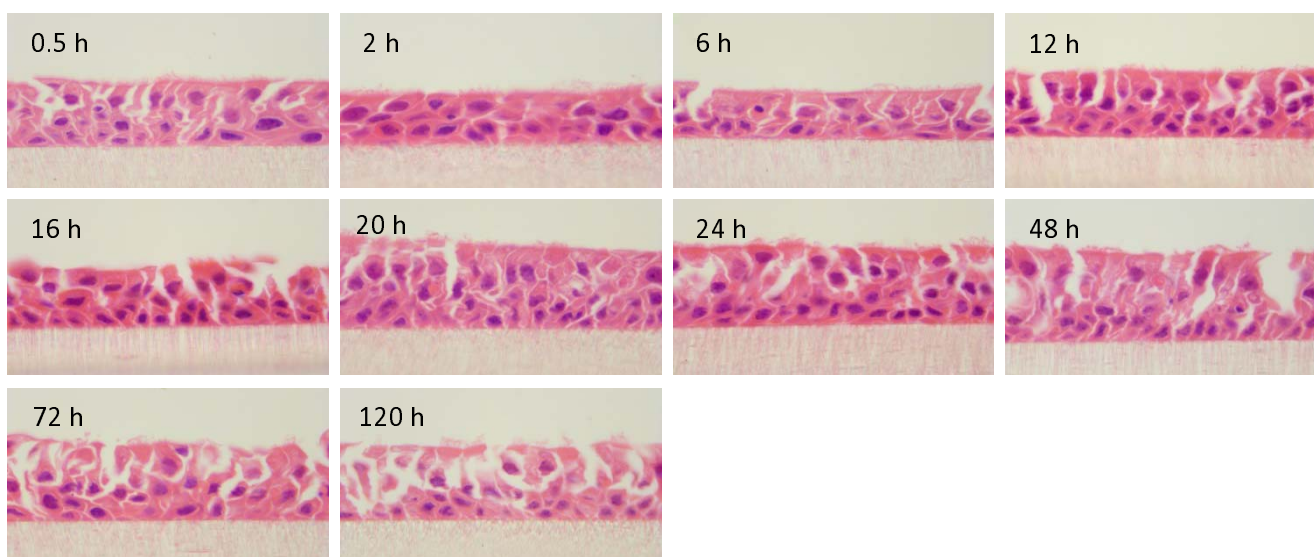
### Uninfected



### PH2

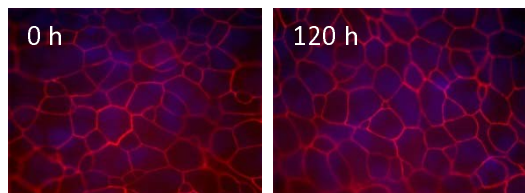


### PH202

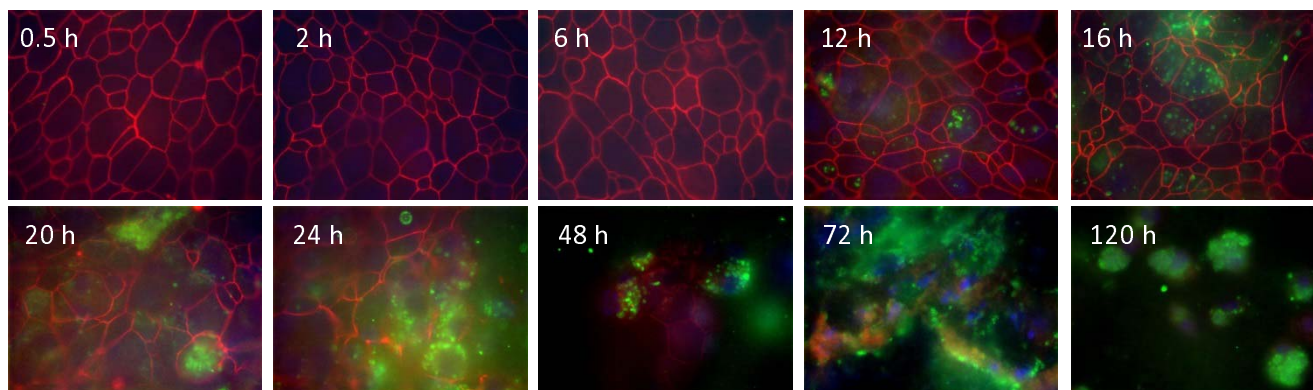


## Supplementary Figure 7

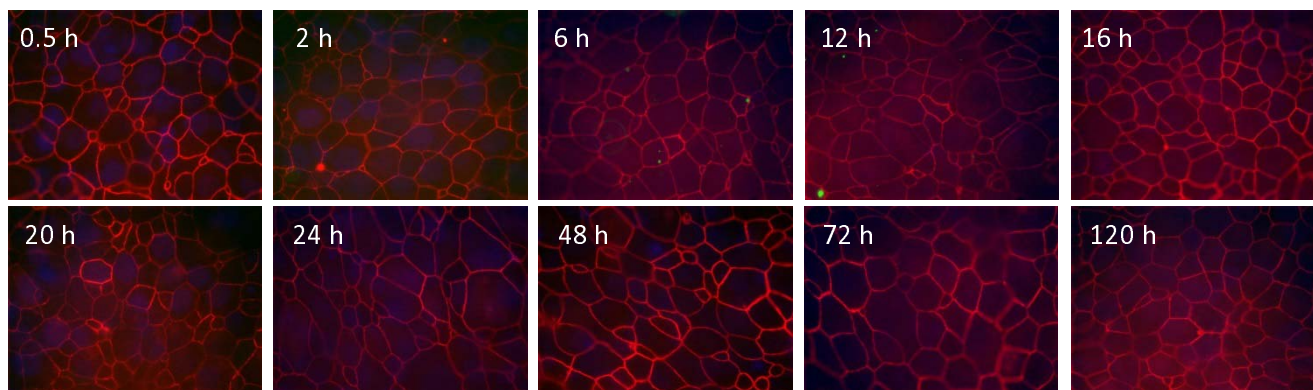
### Uninfected



### PH2

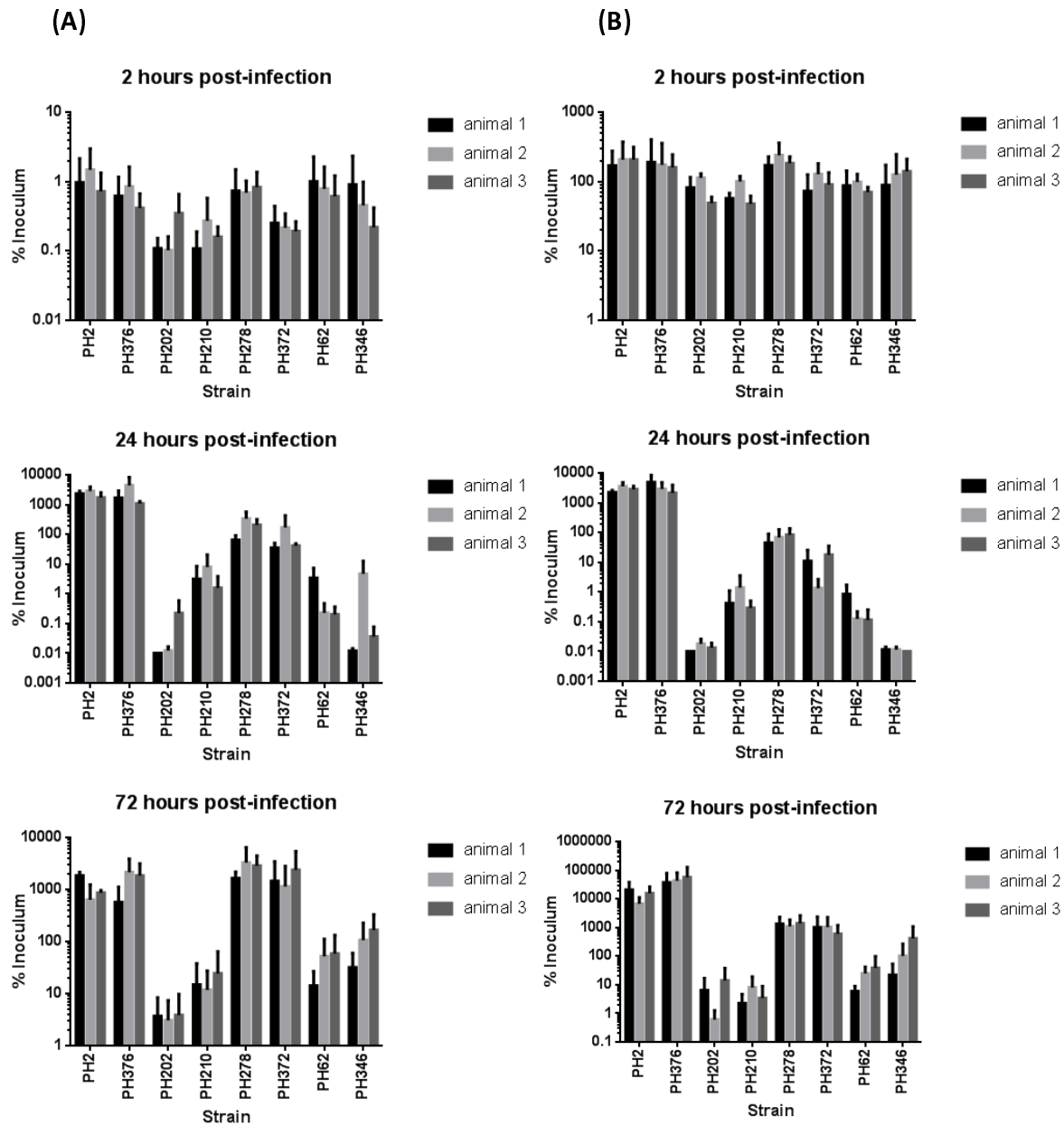


### PH202

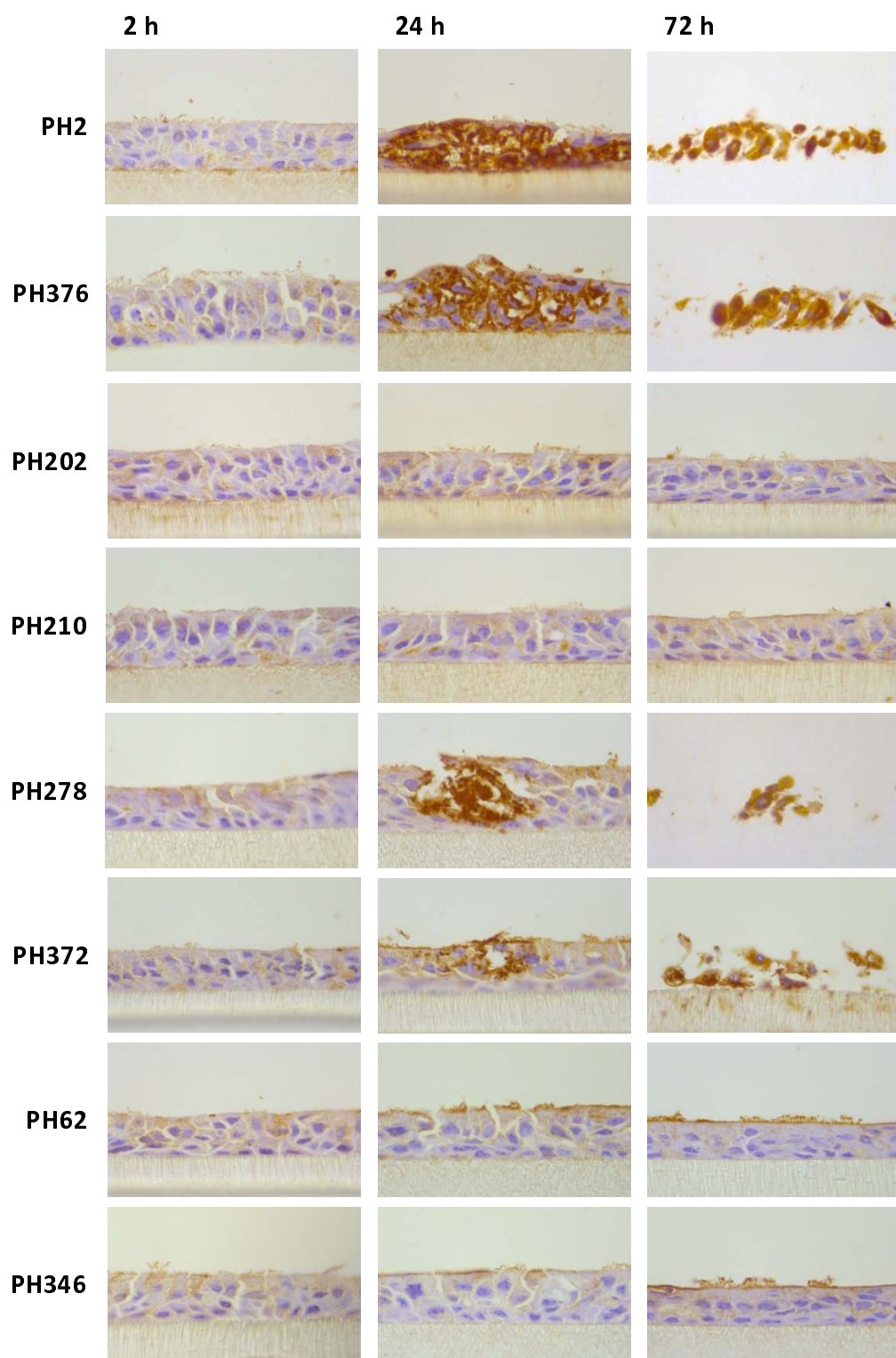




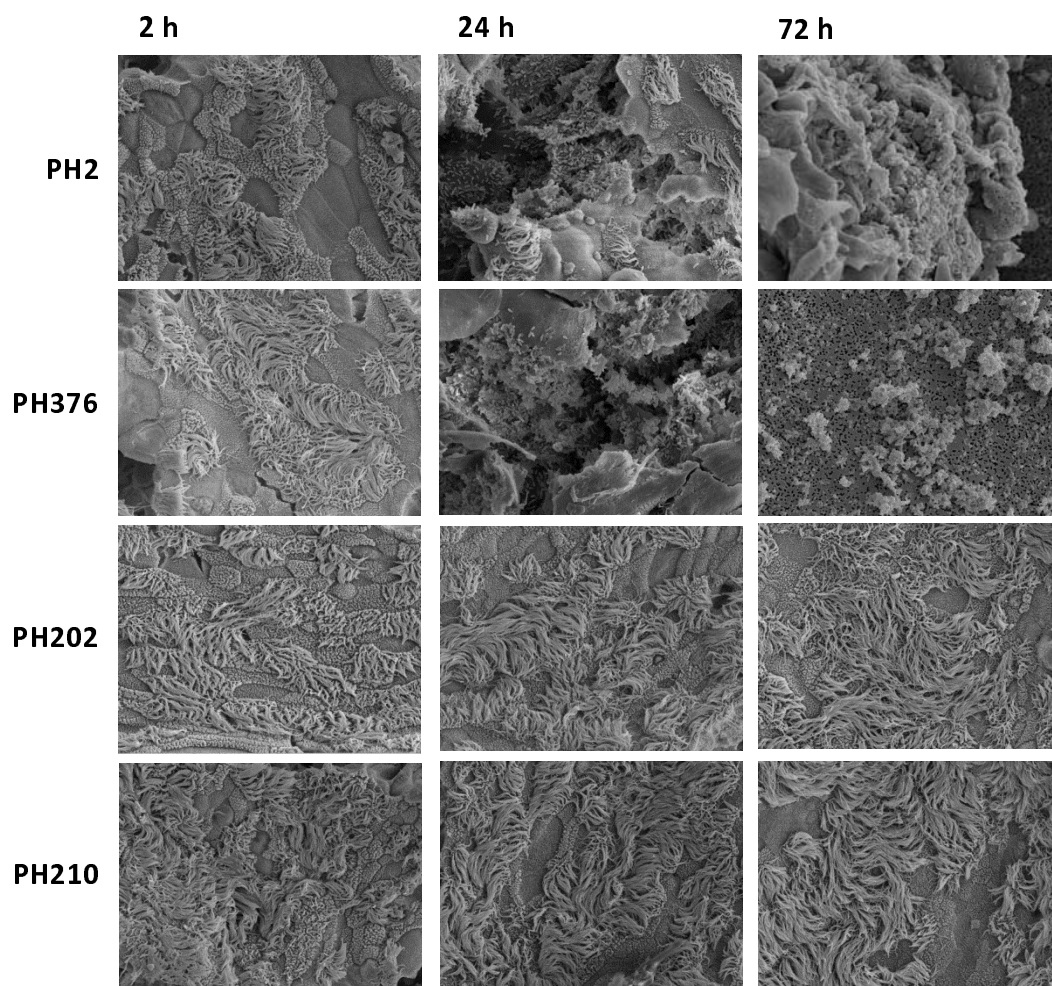
## Supplementary Figure 8



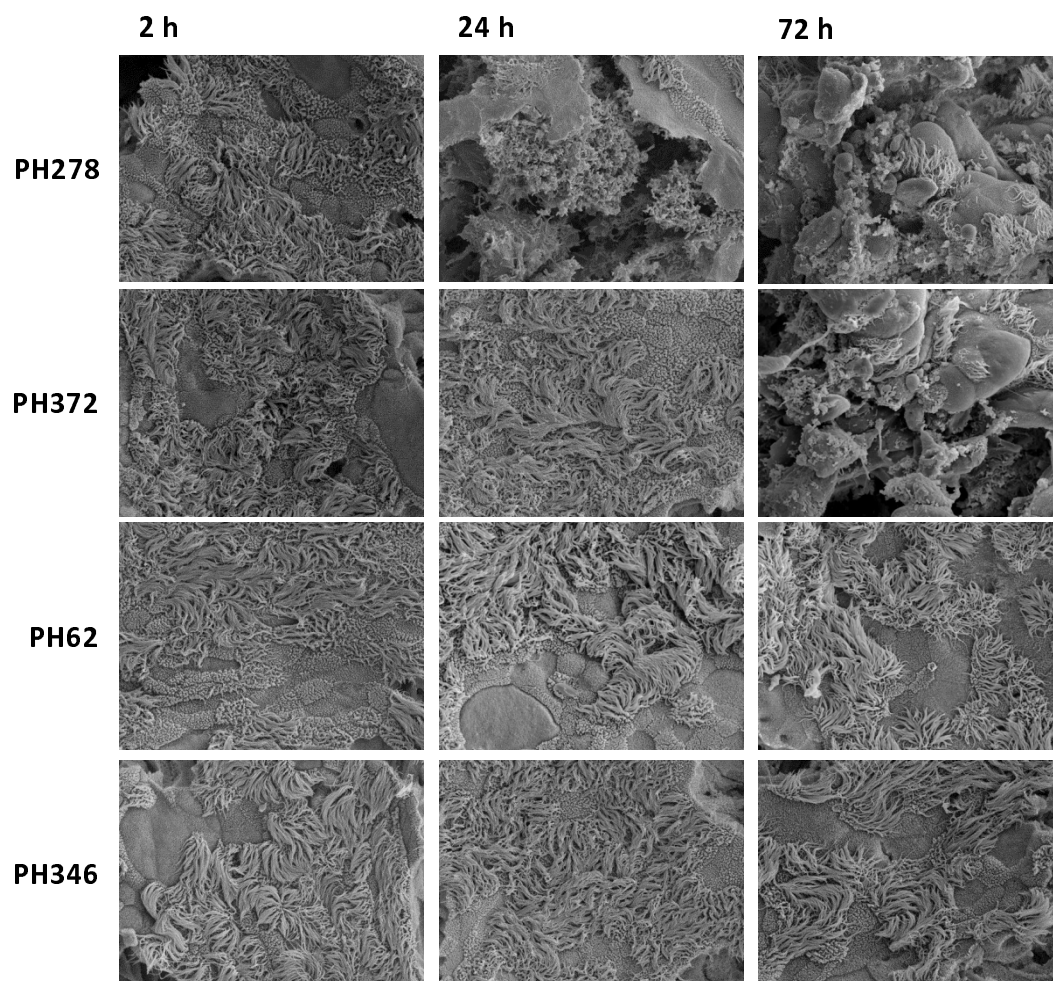
## Supplementary Figure 9



## Supplementary Figure 10



## Supplementary Figure 11



## Supplementary Figure 12

